Downloaded from http://pg.lyellcollection.org/ at Universitetet i Oslo on November 21, 2019

Accepted Manuscript

Petroleum Geoscience

Petroleum geochemical aspects of the Mandawa Basin, coastal Tanzania: the origin of migrated oil occurring today as partly biodegraded bitumen

Tesfamariam Berhane Abay, Katrine Fossum, Dag Arild Karlsen, Henning Dypvik, Lars Jonas Narvhus, Muna Hassan Mohamoud Haid & Wellington Hudson

DOI: https://doi.org/10.1144/petgeo2019-050

Received 19 March 2019
Revised 23 August 2019
Accepted 1 November 2019

© 2019 The Author(s). Published by The Geological Society of London for GSL and EAGE. All rights reserved. For permissions: http://www.geolsoc.org.uk/permissions. Publishing disclaimer: www.geolsoc.org.uk/pub_ethics

To cite this article, please follow the guidance at http://www.geolsoc.org.uk/onlinefirst#cit_journal

Manuscript version: Accepted Manuscript
This is a PDF of an unedited manuscript that has been accepted for publication. The manuscript will undergo copyediting, typesetting and correction before it is published in its final form. Please note that during the production process errors may be discovered which could affect the content, and all legal disclaimers that apply to the journal pertain.

Although reasonable efforts have been made to obtain all necessary permissions from third parties to include their copyrighted content within this article, their full citation and copyright line may not be present in this Accepted Manuscript version. Before using any content from this article, please refer to the Version of Record once published for full citation and copyright details, as permissions may be required.

Downloaded from http://pg.lyellcollection.org/ at Universitetet i Oslo on November 21, 2019

Petroleum geochemical aspects of the Mandawa Basin, coastal Tanzania: the origin of migrated oil occurring today as partly biodegraded bitumen

Tesfamariam Berhane Abay[1*], Katrine Fossum[1], Dag Arild Karlsen[1], Henning Dypvik[1], Lars Jonas Narvhus[1], Muna Hassan Mohamoud Haid[1] & Wellington Hudson[2]

[1] Department of Geosciences, University of Oslo, PO Box 1047, Blindern, NO 0316 Oslo, Norway.

[2] Tanzania Petroleum Development Corporation, PO Box 2774, Dar Es Salaam, Tanzania

*Correspondence: t.b.abay@geo.uio.no

ACCEPTED MANUSCRIPT

Abstract

The shallow marine Upper Jurassic to Lower Cretaceous sedimentary successions of the Mandawa Basin, coastal Tanzania, are located about 80 km away from the offshore gas discoveries of Block 2, Tanzania. In this paper we present petroleum geochemical data, including bitumen extracted from outcrop samples which are relevant to the understanding of the onshore "Petroleum System" and possibly also to the offshore basin. Despite some biodegradation and weathering, common to all outcrop samples, most bitumen samples analyzed contain mature, migrated oil. The maturity span of geomarkers (C_{13}-C_{15} range) covers the entire oil and condensate/wet gas window (Rc = 0.7–2% Rc), with the biomarkers generally indicating the oil window (Rc = 0.7–1.3% Rc). This suggests that the bitumen extracts represent several phases of migrated oil and condensate, which shows that the samples are part of an active or recently active migration regime or "Petroleum System". The source rock facies inferred for the bitumen is Type II/III kerogen of siliciclastic to carbonate facies. This is oil-prone kerogen, typical for a marine depositional system with influx of proximal derived terrigenous material blended in with *in situ* marine algal organic matter (OM). Application of age specific biomarkers

Downloaded from http://pg.lyellcollection.org/ at Universitetet i Oslo on November 21, 2019

such as the C_{28}/C_{29} steranes, extended tricyclic terpane ratio (ETR), nordiacholestanes and the aromatic steroids suggest that more than one source rock have contributed to the bitumen. Possible ages are limited to the Mesozoic i.e. excluding the Late Paleozoic, with the most likely source rock belonging to the Early Jurassic. More geochemical and geological studies should be undertaken to further develop the general understanding of the petroleum system of the Mandawa Basin and its implications to the "Petroleum Systems" both offshore and onshore. This paper also presents a reinterpretation of published gas composition and isotope data on the Pande, Temane and Inhassoro gas fields (Mozambique) with implications for possible oil discoveries in the gas dominated region.

Introduction

Outcrop samples from the Mesozoic Mandawa Basin succession were analyzed with respect to organic content in order to shed light on the petroleum potential of the inferred source rocks and the palaeo-depositional system (Fig. 1). The successions are dominated by siliciclastics with a few carbonate units and evaporites (Aitken 1961; Kent *et al.* 1971; Hudson 2011) (Fig. 2). Bitumen containing samples from the sandstones of these sequences and carbonate rocks representing the Upper Jurassic to Lower Cretaceous Kipatimu Formation and Lower Cretaceous Nalwehe Formation were sampled (Figs 2–4).

The bitumens were extracted and analyzed by several geochemical methods in order to determine and classify bitumen source rocks and the bitumen itself. Challenges of tropical outcrop samples and associated weathering and oxidation of HC-compounds were compounded by generally limited sample amounts, but conclusive results could be establish as presented below. We propose that the data presented may shed light on the oil prospectively of the region, which is still, in terms of exploration, in an early stage.

ACCEPTED MANUSCRIPT

Downloaded from http://pg.lyellcollection.org/ at Universitetet i Oslo on November 21, 2019

Geological setting

General regional setting

The East African coastal basins were formed after the Permo-Triassic (Karoo) rifting event which ended in Late Triassic times. The Karoo sediments were deposited in fairly deep rifts, directly on the Neoproterozoic basement.

Prior to the Gondwana break-up, the Mandawa Basin was located adjacent to Madagascar and the separation of the East Gondwana i.e. Madagascar, India, Antarctica and Australia, relative to the West Gondwana i.e. Africa and South Africa broadly took place along the present day East African coastline (Reeves 2018). A second period of crustal extension was initiated in the Toarcian (Early Jurassic, ca. 180 Ma) which eventually resulted in further break-up and disintegration of Gondwana (Geiger *et al.* 2004; Gaina *et al.* 2013; Reeves 2018). The rift to drift transition commenced in the Middle Jurassic (ca. 170 Ma) with initiation of sea-floor spreading and the opening of the Western Somali Basin and the Mozambique Basin (Eagles & König 2008; Gaina *et al.* 2013). Sea-floor spreading between Madagascar and Africa ceased around 120 Ma and strike-slip motion between Madagascar and India was initiated (Eagles & König 2008; Reeves 2018). In general, such systems can result in anoxic-sub basins due to restriction of circulation patterns. From the Late Cretaceous and into the Early Paleogene, a long period of exceptional stability intervened (Kent *et al.* 1971; Nicholas *et al.* 2007).

Madagascar and the rest of the Eastern Gondwana landmass drifted southwards with respect to Africa, along coast parallel, north-south oriented transform zones, operating between the two spreading centers e.g. the Davie Fracture Zone and Seagap Fault (Fig. 1), cf. Reeves (2018). In particular, the opening of the Indian Ocean and plate movements along the Seagap Fault and Davie Fracture Zone (Fig. 1) were important for sedimentation, influencing directions of sediment transport and also the petroleum geological development of the region (Bosellini 1992; Gaina *et al.* 2013; Sutton *et al.* 2017; Davison & Steel 2018).

The Seagap Fault likely developed as a transform fault during the early stages of oceanic spreading but was later abandoned as the southwards motion of Madagascar was taken up by the Davie Fracture Zone (Sansom 2018), see Fig. 1.

ACCEPTED MANUSCRIPT

Downloaded from http://pg.lyellcollection.org/ at Universitetet i Oslo on November 21, 2019

The offshore area along Tanzanian coastline evolved as a ramp margin from Late Jurassic to Aptian times and is today tectonically structured with several gas fields e.g. SongoSongo (about 15 km offshore) with gas in Lower Cretaceous shelf sands. The end Aptian transgression created a wide, eastwards deepening channelized slope with a narrow shelf to the east with structurally controlled sedimentary entry points (Sansom 2018). Offshore reservoir sandstones in southern Tanzania were deposited by turbidite-contourite systems initiated during Albian times (Siversen *et al.* 2017; Sansom 2018). The Late Aptian transgression was a time of global source rock deposition, where the final separation of Antarctica – Australia from India took place, allowing free oceanic circulation and initiation of contourite currents along the East African margin (Sansom 2018). Reactivation of the Seagap Fault created minor pull-apart basins and pop-up structures which provided structural traps for several of the offshore gas discoveries in Tanzania (Sansom 2018). In general, such effects of inversions and uplift tend to modify the migration regimes for petroleum both in negative and positive ways i.e. uplift allows remigration and phase fractionation (Karlsen & Skeie 2006), and it is possible that the present dominance of gas traps in Tanzania/Mozambique is a result of this effect.

The post-breakup Jurassic and Cretaceous successions of the Mandawa Basin are dominated by shallow marine, coastal to partly terrestrial sedimentation, disrupted by regional breaks and local halokinetic activity (Mbede 1991; Hudson 2011; Hudson & Nicholas 2014), see Figs 2 and 3. Sea level changes, in addition to local tectonics and faulting, were the main factors controlling the regional sedimentological evolution (Kapilima 2003; Hudson 2011; Fossum *et al.* 2018).

Mandawa Basin and East African petroleum geology

Onshore oil seeps, which is a typical feature of active petroleum systems, and also of uplift/tilted regions, have been known for many years in coastal East Africa (Fig. 1), and in a historic perspective did the British E.J. Wayland already in 1925 (Tvedt, 2018, p. 258-260) point to oil seeps in the not too distant rift systems of Lake Albert where Heritage Oil is currently producing oil. Recently, large offshore gas discoveries in Tanzania and Mozambique demonstrated the significant hydrocarbon potential of East Africa, as do heavy oil deposits on the conjugate margin of Madagascar (Boote

ACCEPTED MANUSCRIPT

Downloaded from http://pg.lyellcollection.org/ at Universitetet i Oslo on November 21, 2019

& Matchette-Downes 2009; Muhongo 2013; Purcell 2014; Msaky 2015; Davison & Steel 2018). Oil seeps in the Mandawa Basin (Fig. 1) are found at fault junctions and indicate fracture destruction of hydrocarbon bearing traps by the non-sealed fault facilitating the escape of oil to the surface (Makoye 2016), and possibly also simply less destructive fault reactivation in relation to uplift. Dismigration and remigration of oil in uplift systems result in predictable and significant modifications of several molecular facies and maturity parameters, gas to oil ratio (GOR) and API, in addition to potential blending of oils from different sources (Karlsen & Skeie 2006; Lerch *et al.* 2016a; Abay *et al.* 2017). If not accounted for in the correct manner, such effects can greatly complicate interpretations of organic facies and maturity of migrated bitumen. In that case, erroneous models for petroleum generation, migration and trap evolution results, often with dire consequences for exploration (cf. Karlsen *et al.* 2004).

The petroleum exploration of coastal Tanzania started with the first well in 1954. In 1974 gas of commercial quantities was discovered on SongoSongo Island (Figs 1, 2 and 3) in a Lower Cretaceous reservoir, the Kipatimu Formation. In 1981 gas was found in onshore and shallow offshore reservoirs in the Mnazi Bay (Fig. 1, cf. Muhongo 2013; Msaky 2015).

Geochemical source rock analysis on samples from the SongoSongo-1 well suggests kerogen Type II and III (Mpanju & Philp 1994; Kagya 1996)). In the Mandawa Basin, the onshore Upper Triassic to Lower Jurassic Nondwa Formation salts (Figs 2 and 3) contain organic rich black shales with kerogen Type II and III (Boote & Matchette-Downes 2009; Kagya 1996; Quinton & Copestake 2006).

Recently, several giant offshore gas fields have been discovered a few kms offshore e.g. Tanzania Blocks 1, 2, 3 and 4 (Fig. 1). They contain gas in Upper Cretaceous to Paleogene turbidite/contourite reservoirs. The shales and claystones of the Upper Cretaceous to Paleogene Kilwa Group form well-developed seals (Figs 2 and 3). This far, only gas has been found in the offshore blocks, though apparently with some condensates. Confined amounts of oil have been detected onshore, and three of the onshore Mandawa Basin wells (Mandawa-7, Mita Gamma-1, and Mbate-1, cf. Fig. 1) displayed oil shows (Boote & Matchette-Downes 2009; Quinton & Copestake 2006; Hudson 2011; Siversen *et al.* 2017; Davison & Steel 2018).

ACCEPTED MANUSCRIPT

Downloaded from http://pg.lyellcollection.org/ at Universitetet i Oslo on November 21, 2019

A key issue to the understanding of these petroleum systems is if the discovered gas results from too high maturities of the kerogen, in which case the source rock is "burnt out" for oil, or if the limiting factor to oil occurrences in the region is in fact a predominantly gas generative kerogen. Alternatively, it could be that gas has transposed or remigrated oil up-dip by displacement (cf. Gussow, 1954; Sales, 1997), a common process in generative basins. In the latter case, the gas occurrence in the fields is not diagnostic criteria concerning the potential oil-generative capability of the source rocks, and it can accordingly not be ruled out that there is oil, e.g. down-dip or up-dip. Thus, there is a clear need for geochemical investigations of the oil and gas in the region, to provide a comprehensive model for the migration regime, and a study of potential oil inclusions in the traps which are today holding gas, could shed light on the filling history of the trap system (cf. Karlsen *et al.* 1993, 2004).

Wilkin (2017) and Sullivan & Lawson (2017) classified the offshore Tanzanian gas as dry with 97–98% CH_4 and quite mature by applying compositional and carbon isotope analysis. Their results indicated Type III kerogen to be the source for the gas with a possible Middle to Upper Jurassic age. Burial temperatures of up to 180–200°C, i.e. gas-window maturities, were indicated to the north and south of the Mandawa Basin, while in the Mandawa Basin, apparently much lower temperatures and maturities seem to prevail.

An important contribution with respect to the "super-national" petroleum systems of this region is a geochemical study by Loegering & Milkov (2017) on thermogenic gas from fields onshore Mozambique which may have implications also to petroleum systems on- and offshore Tanzania. According to this study, the Inhassoro, Pande and Temane gases are relatively dry, dominated by isotopically light methane, and the gas systems were concluded to be non-biodegraded and of high maturity. This is important as the source rocks are thus inferred to be over mature with respect to oil generation. If correct, this could mean a reduction in the oil-potential of the region.

Still, a review by us of the published data leads us to conclude that the gas is severely biodegraded and it is clear that the butane isomers do not follow the "thermodynamically- ordered-intermolecular-carbon-isotope-distribution" (cf. Galimov 1973; Galimov 1985), and the molecular ratios of iso-butane to n-butane deviates severely from the universal 0.45 to 0.55 ratio of virgin thermogenic HC-gas systems

ACCEPTED MANUSCRIPT

Downloaded from http://pg.lyellcollection.org/ at Universitetet i Oslo on November 21, 2019

(Fig. 5). Hence the gas is irrefutably biodegraded and is in fact isotopically too heavy due to biodegradation and not due to high source rock maturity.

The $\delta^{13}C$ methane values reported are clearly influenced by both methane oxidation and early diagenetic methane genesis as typical for such shallow traps. We suggest the gases not to be over-mature, but rather that the gases are oil associated (cf. Schoell 1983), i.e. generated together with oil at a maturity of about 0.8 to 0.9% Rc (cf. Whiticar 1994 for relationship between $\delta^{13}C$ and maturity), and the source rock system is thus oil-mature i.e. inside the oil-window, and not over-mature. This, if correct, has huge implications to oil exploration in the region. Clearly more research is needed imminently, as in fact the basins could have been written off as gas-generative, when they in fact are also oil generative. It could just be that effects of migration has resulted in traps found using the current exploration model, are the gas part of the total petroleum system. In Norway, historically, parts of the Halten Terrace were similarly written off as gas generative. We proved oil to be generated there, and could show that the condensates and oil were in fact sourced from the same source rock at the same maturity (Karlsen *et al*. 2004; Karlsen & Skeie 2006).

Severe vertical PVT-induced fractionation during migration affected the API and GOR of the reported condensates and some of the maturity parameters, which would then be reported as too high (cf. Karlsen & Skeie, 2006). This example could serve to illustrate the significance of understanding the physio-chemical processes of migration and the effects of biodegradation. The implications of this effect and its consequences to oil exploration in the study region are self-evident.

In the onshore Ruvu Basin, 50 km west of Dar es Salaam, approximately 2.7 tcf gas was discovered in 2015 in the Mambakofi-1 well (Whaley 2016). The Mambakofi-1 well is 3000 m deep, terminating in Triassic formations. The gas was found in Upper Cretaceous sandstones and the source rock is presumably Upper Jurassic shales. In addition, a gas column has been detected in the Mbuyu-1 well which is believed to have hit a new Triassic play (Whaley 2016).

Along the North Eastern Mozambique coastline from the Zambezi delta in the south to the Rovuma Basin and into Tanzania waters (Mafia Basin – offshore portion of the Mandawa Basin) in the north (Fig. 1), several giant gas fields have been found and

ACCEPTED MANUSCRIPT

Downloaded from http://pg.lyellcollection.org/ at Universitetet i Oslo on November 21, 2019

more are anticipated (Davison & Steel 2018). The Mozambique authorities hope for a start of gas production in 2022 (Palermo *et al.* 2014).

In the Rovuma and Angoche basins (south of Rovuma) a Jurassic source rock has been suggested, with Upper Jurassic to Cretaceous reservoirs of submarine turbidity fan and channel affinity. This is comparable to what has been described from other offshore Mozambique sites farther south, and in Tanzania and Kenya in the north (Mahanjane *et al.* 2014; Barlass *et al.* 2017; Davison & Steel 2018, see Fig. 1).

Mahanjane *et al.* (2014) claim that the gas in the Angoche Basin was formed by cracking of original Jurassic sourced oil, while Loegering & Milkov (2017) argue that the onshore gas of Mid Mozambique (Pande, Temane and Inhassoro fields) most likely was derived from the Upper Cretaceous Domo Shale. Thus, considerable dispute and uncertainity still exist concerning the petroleum system (s) of the region, and work is needed for clarification. Concerning cracking, detailed investigations of pyrobitumen resulting from oil cracking should in that case exist, but oil stability is much higher than commonly assumed, and oil will not crack to dry gas in a reservoir at temperatures of 180–200^{o}C (Karlsen & Skeie 2006). A recent paper by Zhonghong *et al*. (2019) demonstrates oil stability at 7 km depth in the Tarim Basin (NW China) with no evidence for cracking.

Onshore Mandawa Basin geology

The Upper Triassic Mbuo Formation is the oldest sedimentary succession in the Mandawa Basin (Figs 2 and 3), comprising conglomerates, sandstones and claystones of alluvial, fluvial and lacustrine affinity. The area between the Matandu and Mbwemkuru lineaments (Fig. 2) was occupied by lakes and swamps during Late Triassic to Early Jurassic times (Hudson 2011). The Mbuo claystones (Figs 2 and 3) were deposited in lagoonal settings, and the organic rich claystones are presently recognized with a good source rock potential (Hudson 2011; Hudson & Nicholas 2014). As crustal extension continued at the end of the Triassic, marine incursions created restricted marine environments and hypersaline lakes in central parts of the Mandawa Basin. Sea water periodically entered the coastal lakes and created hyper-saline environments, and finally the Nondwa Formation evaporites (Figs 2 and 3) were deposited. The restricted environment allowed organic matter to be preserved in a sub-oxic to partly anoxic environment, thus creating organic rich shales with

ACCEPTED MANUSCRIPT

Downloaded from http://pg.lyellcollection.org/ at Universitetet i Oslo on November 21, 2019

good/fair source rock qualities (Kagya 1996). After the separation of East and West Gondwana the general regional depositional environment can be characterized as shallow to marginal marine. The Mitole and the Nalwehe formations (Figs 2 and 3) consist of marine limestones overlain by prograding sandstones, while the overlying Kihuluhulu Formation was deposited in open shelf settings (Mpanda 1997; Hudson 2011; van Den Brink 2015; Haid 2018).

The depositional conditions varied in the northern part of the Mandawa Basin during Late Jurassic. The Kipatimu Formation, which is only found in a relatively underexplored area north of the Matandu River (Fig. 3), is poorly understood compared to related formations in central and southern part of the Mandawa Basin. The Kipatimu Formation represents mainly terrestrial, fluvio-deltaic depositional conditions consisting of alternating massive red sandstones (often cross-bedded) intercalated with purple to greenish claystones and some occasional conglomerates (Stockley 1943; Aitken 1961; Kent *et al.* 1971; Hudson 2011; Gundersveen 2014). The Kipatimu Formation cannot be directly correlated with any particular unit in southern and central Mandawa Basin (Aitken 1961). The age of the Kipatimu Formation in the Mandawa Basin has not fully been resolved, but a Late Jurassic age seems likely (Hudson 2011; Msaky 2015; Smelror *et al.* 2018). The Kipatimu Formation is overlain by Lower Cretaceous clays and sandstones (Figs 2 and 3). Lower Cretaceous part of the Kipatimu Formation is assumed missing in the Mandawa Basin, but is found onshore in the Rufiji Basin to the north, and in offshore boreholes.

ACCEPTED MANUSCRIPT

Previous geochemical studies

Oil seeps and bitumen extracted from Tanzanian outcrops and wells were analyzed by Mpanju & Philp (1994). In this respect the Wingayongo seeps in the Rufiji Basin (north of the Mandawa Basin) are of particular importance (Figs 1 and 3). Oil seeps in the Wingayongo area represents migration through regional faults and the topmost 40 m of the Lower Cretaceous Kipatimu sandstones are stained with bitumen in the Wiangongo-1 borehole. The oil saturated sandstones point to an oil-prone source at depth, possibly Bajocian shales (Mpanju & Philp 1994).

Downloaded from http://pg.lyellcollection.org/ at Universitetet i Oslo on November 21, 2019

Kagya (1996) studied the geochemical signatures of Triassic shales and evaporites (Nondwa Formation, Figs 2 and 3) in the Mandawa-7 test well (Fig. 2). The Triassic section of the Nondwa Formation displays TOC values in the range from 1.23 to 7.41 wt%, and kerogen of Type II to III. The depositional environment was at times hypersaline, as reflected by the presence of C_{24} tetracyclic terpanes, gammacerance and C_{35} homohopanes (Kagya 1996). Varied abundances of C_{27}- C_{28}- C_{29}- steranes suggest mixed organic input from marine and terrestrial sources, representing marine to estuarine depositional conditions (Kagya 1996).

Mkuu (2018) evaluated the thermal maturity levels of Cretaceous to recent sedimentary succession from the Mafia Island and SongoSongo Island boreholes (Fig. 1). TOC values for the Kipatimu Formation in the Mafia borehole (Msufi-1) varies between 0.1 and 0.8 wt%, while that of the SongoSongo samples (Mtiki-1 and Mkongo-1 wells) range between 0.3 and 3 wt%. The Kipatimu Formation was penetrated in all three wells, and the maturity levels were found to be well within the oil window (Mkuu 2018).

In the Mafia borehole, the Kipatimu Formation is present down to 5600 meter depth and vitrinite reflectivity values range from 1.6 to 2.9% Ro (mainly the dry gas zone), whereas the overlying succession has vitrinite reflectivity values in the range of 0.3 to 1.3% Ro. In the Mtiki-1 well at SongoSongo Island, the Kipatimu Formation was encountered between 1300 to 2050 meter burial depths, and the vitrinite reflectance values between depths of 1508 to 2018 meter indicate mostly early to late stages of liquid hydrocarbon generation (0.5 to 1.0% Ro). The overlying successions are thermally immature (0.2 to 0.3% Ro). The Kipatimu Formation of Mkongo-1 was encountered between 1800 and 2086 meter. Below 1950 meters depth the window for early liquid petroleum generation appears. The geothermal gradients were estimated to be 42°C and 37°C for the Mafia and the SongoSongo Island, respectively. It is clear that these relatively moderate gradients and the depth of the oil window suggest that uplift has affected this region, thus a gas driven remigration event may have post-dated the most recent petroleum generative phase.

ACCEPTED MANUSCRIPT

Downloaded from http://pg.lyellcollection.org/ at Universitetet i Oslo on November 21, 2019

Sample set and methods

The analyzed outcrop samples were collected during fieldwork in the Mandawa Basin in 2014 (Figs 1 and 2). All geochemical analyses performed in this study conform to the Norwegian Industry Guide to Organic Geochemical Analyses (Weiss *et al.* 2000).

Six sandstone samples from the Kipatimu Formation in north Mandawa (WP92 section, Figs 1, 2, 3 and 4; Table 1) were analyzed geochemically. The sampled section span the Jurassic – Cretaceous boundary with a transgressive conglomerate horizon separating the two units (Fig. 4).

Samples WP92-5-14 and WP92-7-14 were collected from the Upper Jurassic part of the Kipatimu Formation, while samples WP92-11-14, WP92-13-14, WP92-16-14 and WP92-19-14 likely represent the Lower Cretaceous Kipatimu Formation (Fig. 4).

Two sections (NQ1 and NQ2) representing the Lower Cretaceous Nalwehe Formation were sampled from the northern culmination of the Mandawa Dome (Figs 2, 3 and 4). Three samples (NQ1-1-14, NQ1-3-14 and NQ1-7-14) were sampled from the NQ1 section (Fig. 4; Table 1). Samples NQ1-1-14 (mudstone) and NQ1-3-14 (wackestone) belong to the Nalwehe Limestone Member, while sample NQ1-7-14 is a sandstone from the Nalwehe Sandstone Member, cf. Figures 3 and 4; Table 1. In addition, sample NQ2-2-14 was collected from the Nalwehe Limestone Member from the NQ2 section (Fig. 4).

In addition, two Lower Cretaceous sandstone samples from the Southern Mandawa Basin were analyzed: MKW-1-14 and MKW-5-14 (Figs 2, 3 and 6; Table 1). The stratigraphical position of these samples has not fully been resolved but they are tentatively assigned to the Nalwehe Formation (Haid 2018). Furthermore, a sample (HTQ) from the Hoteli tatu gypsum quarry (see Fig. 2 for sample location) was included. This sample was collected from an interbedded gypsum and shale from the Lower Jurassic Nondwa Formation (Figs 2-4).

The outcrop samples were collected in the coastal areas, in forests and along road cuts, in a sub-Sahara climate of generally high air temperatures and highly variable humidity. Consequently, there may have been significant depletion of organic matter in the rock samples due to weathering, biodegradation, evaporation and water washing (cf. Tissot & Welte 1984). The rock samples may also have been

ACCEPTED MANUSCRIPT

Downloaded from http://pg.lyellcollection.org/ at Universitetet i Oslo on November 21, 2019

contaminated by exhaust fumes and engine oil from passing cars. Non-geological factors of this kind could affect the geochemical signatures recorded by standard analytical techniques, increasing the uncertainty of the geochemical interpretation (Abay *et al.* 2017). Despite these obstacles, quantification of key organic facies and maturity parameters proved to be possible (Tables 2 and 3).

Further detailed descriptions of localities and lithology plus stratigraphy are presented in Appendix 1.

Extraction of organic matter

The rock samples were crushed to powder in a steel mill before extraction of soluble bitumen. A Soxtec system HT 1043 was used to extract the bitumen from the powdered samples. The extraction solvent was a mix between 93 vol% dichloromethane (DCM) and 7 vol% methanol (MeOH), Karlsen & Larter 1991. Activated copper grains were used to remove elemental sulphur (Weiss *et al.* 2000). The samples were boiled for 1 hour and the condensing solvent was subsequently rinsed for 2 hours. After extraction, the samples were carefully concentrated by evaporating the excess solvent in air at room temperature to prevent loss of the analyte.

Rock-Eval pyrolysis and TOC analysis

The samples were screened for source quality by measuring their total organic carbon (TOC) and determining key Rock-Eval parameters. Carbonate was removed from the crushed samples by diluted hydrochloric acid prior to TOC analysis. Total organic carbon was then determined by combustion. A Leco CS-632 combustion instrument was used for the TOC analysis. Rock-Eval pyrolysis was carried out using a HAWK instrument.

Gas chromatography – flame ionization detection (GC-FID)

The bulk rock extracts were analyzed using a Varian capillary gas chromatography–flame ionization detector (GC-FID) Model 3800, with a 25 m long Hewlett Packard Ultra II cross-linked methyl silicone column (0.2 mm inner diameter, film thickness 0.33 µm). The initial temperature for the chromatographic column was 40°C, which

ACCEPTED MANUSCRIPT

Downloaded from http://pg.lyellcollection.org/ at Universitetet i Oslo on November 21, 2019

was held for 2 min. Subsequently, the column was heated with a gradient of 4.5°C until it reached a final temperature of 320°C, which was held for 20 min.

Gas chromatography – mass spectrometry (GC-MS/MS)

Normal alkanes (n-alkanes) are usually much more abundant than biomarkers in any standard GC-MS analysis so their signature tends to override that of the associated biomarkers. To prevent this, the n-alkanes were removed by sieving using a 5 Å molecular sieve so as to increase the relative strength of the biomarker signatures (Karlsen et al. 1993). Biomarkers were subsequently analyzed using a Thermo Scientific TSQ Quantum XLS triple-quadrupole mass spectrometry (GC-MS/MS) with a 60 m long polar fused silica column. The column had an inner diameter of 0.25 mm and a film thickness of 0.25 µm.

The GC-MS/MS was set to an initial column temperature of 40°, held constant for 1 min. The temperature was followed a gradient of 10°C/min to 180°C and then at 1.7°C/min to 310°C, and held for 40 min. Ions with mass to charge ratios (*m/z*) of 142, 156, 170, 178, 191, 192, 198, 217, 218, 231 and 253, and parent–daughter transitions, such as *m/z* 358 → 217 and *m/z* 372 → 231 were recorded.

Results and Discussion

Total organic carbon (TOC) and Rock-Eval pyrolysis were performed for source rock screening and to determine if the bitumen in the samples is *in-situ* or migrated (Table 2; Fig. 7). Normal alkanes, isoprenoids, medium ranged hydrocarbon compounds, as well as saturated and aromatic biomarker parameters from GC-FID and GC-MS analyses were used to determine the facies, thermal maturity levels and likely age of the bitumen in the analyzed samples (Table 3; Figs 8–17).

TOC and Rock-Eval pyrolysis

The aim of this section is to present geochemical evidence on the origin of the petroleum compounds in the samples. The section will show that most of the samples analysed consist of migrated petroleum in contrast to *in-situ* generated petroleum. The source rock potential of rocks can be assessed based on total organic carbon (TOC, wt%) and S2 Rock-Eval data (mg HC/g rock), cf. Tissot & Welte (1984) and

ACCEPTED MANUSCRIPT

Downloaded from http://pg.lyellcollection.org/ at Universitetet i Oslo on November 21, 2019

Peters & Cassa (1994). According to the combustion analysis, the TOC values range from 0.01 to 1.13 wt% (Table 2). Considering a minimum TOC value of about 0.3 wt% for carbonate and evaporitic sediments, and about 0.5 wt% for detrital/clastic rocks (Tissot & Welte 1984), only two samples (NQ1-3-14 and NQ2-2-14) (Table 2) could tentatively be considered potential source rocks, and these values are today considered minimum values. This overall poor source rock potential of the samples is also supported by the extremely low Rock-Eval S2 (0.02 to 0.32 mg/g rock) and HI (6 to 177 mg HC/g TOC) values (Table 2). From this it is clear that the kerogen type in the samples is mostly Type III/IV and that the samples are not source rocks by any commercial criteria.

The TOC contents of samples WP92-5-14, WP92-7-14, WP92-13-14, WP92-16-14, WP92-19-14 (sandstones from the Kipatimu Formation of the WP92 section) and NQ1-7-14 (sandstone from the Nalwehe Sandstone Member of the NQ section) and MKW-1-14 and MKW-5-14 (sandstones from the MKW section) (Fig. 4) are between 0.01 wt% and 0.06 wt%, just below detection limits. The TOC for these samples are so low that the related results of the Rock-Eval pyrolysis are very uncertain. Such low TOC values are not uncommon in sandstone samples that may contain allochthonous (migrated) petroleum as opposed to an *in situ* content. Samples containing migrated petroleum can be distinguished from those containing *in situ* bitumen by comparing their production indices (PI), which is expressed by a ratio between the free hydrocarbon (S1) and the remaining hydrocarbon generating potential (S2) (PI = S1/S1+S2). The S1 values for the sample set are very low and range between 0.01 and 0.06 mg HC/g rock. However, Figure 7 displays a number of the samples showing PI values higher than 0.40, commonly used as cut-off value to signify migrated petroleum (e.g. Tissot & Welte 1984; Hunt 1996). This interpretation is also supported by the described low TOC and HI values of the samples, which suggests that *in situ* generation of petroleum is, for most of the samples, low to moderate. In particular, the following samples show clear-cut evidence of migrated petroleum: MKW-1-14, NQ1-7-14, WP92-5-14, WP92-7-14, WP92-13-14 and WP92-16-14 (Fig. 7; Table 2).

It should be noted that tropical surface samples like these normally would have experienced significant evaporation of hydrocarbon compounds, otherwise appearing as S1. Biodegradation of hydrocarbon compounds in porous surface samples is also

ACCEPTED MANUSCRIPT

Downloaded from http://pg.lyellcollection.org/ at Universitetet i Oslo on November 21, 2019

a common reason for reduced S1 values. Furthermore, a complication also exists since biodegraded petroleum or heavy oil compounds like asphaltenes may appear as S2 on the Rock-Eval (Karlsen & Larter 1989; van Koeverden *et al.* 2010; Abay *et al.* 2017), which also will lower the PI. This suggests that the petroleum in most of the sandstone samples, including those with PI lower than 0.4, can be considered as migrated petroleum. Additional evidences for migrated petroleum can be found in the GC-FID chromatograms, in which case a mature profile of n-alkanes without a clear biomarker hump at the C_{30}-C_{35} alkane interval is evident (Abay *et al.* 2017). The GC-FID chromatograms of samples WP92-13-14 and MKW-5-14 (Fig. 8) clearly display this phenomenon. The unresolved complex mixture (UCM, Fig. 8) hump under the C_{15}–C_{30} n-alkanes indicates biodegradation, and this furthermore strengthens the presence of migrated petroleum in these sandstone samples, as petroleum in such samples are prone to biodegradation compared to petroleum in a tighter shale/clay source rock lithology, which cannot be biodegraded.

The presence of migrated petroleum in such samples is often corroborated by low T_{max} values (mostly lower than about 435°C) as known from numerous worldwide investigations (e.g. Peters 1986). However, caution should be observed when interpreting T_{max} values associated with confined S2 <0.2 mg HC/g rock (Peters 1986), which is the case for most of the present samples. Two of the analyzed samples (i.e., NQ2-2-14 and HTQ1-14) yielded S2 values of 0.21 and 0.32 mg HC/g rock, respectively, and their respective T_{max} values, 434°C and 366°C, may thus be regarded reliable and in line with migrated petroleum.

Normal alkane and isoprenoid distribution patterns

Data from GC-FID are used as indicators of depositional environment and maturation of source rocks. However, these data are also among the first to be affected by alteration processes such as biodegradation and by contamination, unlike biomarkers, which mostly survive such effects. Therefore, being aware of these problems is an important aspect when interpreting such data especially of surface samples. The pristane/n-heptadecane (Pr/n-C_{17}) and the phytane/n-octadecane (Ph/n-C_{18}) ratios for the samples analyzed range from 0.24 to 16.6 and 0.09 to 1.08, respectively, while the pristane/phytane (Pr/Ph) ratios varies greatly and range from 0.09 to more

ACCEPTED MANUSCRIPT

Downloaded from http://pg.lyellcollection.org/ at Universitetet i Oslo on November 21, 2019

than 10 (Table 3; Fig. 9). These ratios are used to estimate the redox conditions of source rocks during their deposition, and to indicate the OM type (e.g. Didyk *et al.* 1978). The ratios may, however, be affected by other factors such as maturation and bacterial degradation (Peters & Moldowan 1993). Some of the extremely high ratios of Pr/n-C_{17}, Ph/n-C_{18} (see Fig. 9) and Pr/Ph derived from the quantifications of the GC-FID chromatograms can be due to contamination and/or poor signal-to-noise ratio. Note that the GC-FID traces, which display mainly saturated hydrocarbon compounds are, in our study, less reliable compared to the GC-MS data. This is common for surface samples, biodegraded samples and contaminated samples as all organic constituents including contaminants appear in the GC-FID traces. In contrast, GC-MS analysis monitors specific biomarker compounds based on the preferred mass to ion (*m/z*) ratio. Many contaminating compounds are also removed along with n-alkanes during the molecular sieving process, which was carried out prior to the GC-MS analysis.

Still, we conclude that the GC-FID data (n-alkanes and isoprenoids), and the presence of an UCM, appear to be useful and are used in combination with the GC-MS data to assess the organic facies, maturity and biodegradation (Figs 8 and 9).

Saturated hydrocarbon maturity and organic facies parameters

Several organic facies, maturity and age related parameters of saturated hydrocarbons have been calculated from the GC-MS chromatograms of terpanes (*m/z*=191) and steranes (*m/z*=217), and a list is presented in Table 3.

From *m/z*=191 mass chromatograms (Fig. 10), it can be seen that the hopanes are fully isomerized meaning that the maturity is higher than 0.5% Ro (e.g. Peters *et al.* 2005). The 22S/(22S + 22R) ratio of the C_{31} hopane for the investigated samples ranges from 0.58 to 0.68 (Table 3), i.e. more or less 0.6 and slightly higher than the equilibrium value for this parameter (Peters *et al.* 2005) , giving a maturity of (0.55–0.65% Ro). This ratio does not increase further throughout the oil and gas window.

The 18α(H)-22,29,30-trisnorneohopane (Ts) to 17α(H)-22,29,30-trisnorhopane (Tm) ratio, Ts/(Ts + Tm) (Seifert & Moldowan 1978) is reliable maturity parameter with a large dynamic range, which extends until the end of the oil window. The Ts/(Ts + Tm)

ACCEPTED MANUSCRIPT

Downloaded from http://pg.lyellcollection.org/ at Universitetet i Oslo on November 21, 2019

ratio for the investigated samples varies from 0.34 (sample NQ1-1-14) to 0.59 (sample MKW-1-14) (Table 3; Fig. 11), suggesting early to medium mature bitumen or oil (Seifert & Moldowan 1978; Peters *et al.* 2005). More specifically, samples MKW-1-14, MKW-5-14, WP92-13-14, WP92-16-14, WP92-7-14 show (Ts/Ts + Tm) values in the range of 0.43–0.59, while samples NQ1-1-14, WP92-19-14 and WP92-11-14 show value between 0.34 and 0.39 (Table 3; Fig. 11).

The maturity of the samples MKW-1-14, MKW-5-14, WP92-13-14, WP92-16-14, and WP92-7-14 is consistent with that of Karlsen *et al.* (1995) who reported Ts/(Ts + Tm) values in the range of 0.5 to 0.7 for a dataset consisting of 33 oils from Mid-Norway. These Mid-Norway oils are concluded to have a maturity corresponding to 0.8–1.2% Ro (Karlsen *et al.* 1995). The Ts/(Ts + Tm) values for samples NQ1-1-14, WP92-19-14 and WP92-11-14 are slightly below the transition from immature sediments into the oil window zone, which commences at a Ts/(Ts + Tm) value of 0.4 (Abay *et al.* 2017). While such low Ts/(Ts + Tm) ratios may indicate an immature nature of the samples, the ratio should be used with great caution because it is strongly influenced by source rock facies. Thus, several authors including McKirdy *et al.* (1983), Rullkotter *et al.* (1984) and Peters *et al.* (2005) reported that oils from carbonate source rocks show low Ts/(Ts + Tm) ratio compared with those from clay or shale. Consequently, some of the low Ts/(Ts + Tm) ratios, typically that of NQ1-1-14, which is a limestone, and probably that of WP92-19-14, could reflect such an association.

The diahopane/(diahopane + normoretan) ratios for the samples range from 0.11 to 0.70 (Fig. 12; Table 3). According to Karlsen *et al*. (1995), diahopane/(diahopane + normoretane) ratios in the range from 0.5 to unity are typically associated with migrated petroleum. However, care should be taken as increased amount of diahopane could also indicate higher terrestrial input (e.g. Lerch *et al.* 2016a).

The 29Ts/(29Ts + norhopane) parameter is not susceptible to any source rock facies effect we know of, and is a very robust maturity parameter (Moldowan *et al.* 1991; Karlsen & Skeie 2006). The 29Ts/ (29Ts + norhopane) ratio for the samples analyzed lies between 0.16 and 0.39 (Table 3; Fig. 11) and this corresponds roughly to c. 0.8 to 1.2% Rc (Karlsen *et al.* 1995), based on their 33 oils and condensates from the Norwegian Continental Shelf, reported 29Ts/ (29Ts + norhopane) ratios between 0.2 and 0.4, in agreement with the results of this study. The relatively low values of

ACCEPTED MANUSCRIPT

Downloaded from http://pg.lyellcollection.org/ at Universitetet i Oslo on November 21, 2019

29Ts/(29Ts + norhopane) in the WP92-11-14 and WP92-19-14 samples of this study possibly represent a span from *in situ* generated bitumen, to clearly migrated petroleum. The notion that *in situ* generated petroleum is present is also supported by the low Ts/(Ts +Tm) ratio and by the fact that these samples (WP92-11-14 and WP92-19-14) do not contain migrated petroleum as indicated by the Rock-Eval data (Fig. 7).

The close-to linear correlation between the 29Ts/(29Ts + norhopane) versus Ts/(Ts + Tm) suggests that any source rock facies effect on these parameters is minor to non-existent (Fig. 11). Higher maturity is clearly observed for the samples MKW-1-14 and MKW-5-14, followed by the NQ1-7-14, WP92-13-14, WP92-7-14, WP92-16-14, WP92-5-14, with the WP92-11-14 and WP92-19-14 samples making up the least mature samples in the set (Fig. 11).

Figure 11 in general supports the notion that both the 29Ts/(29Ts + norhopane) and Ts/(Ts + Tm) increase with maturity. Still, sample NQ1-1-14, an outlier in Figure 11, shows relatively high maturity with respect to 29Ts/(29Ts + norhopane), while the Ts/(Ts + Tm) ratio suggest low maturity. This discrepancy corroborate with the presence of carbonate-related source rock in sample NQ1-1-14.

With increasing maturity, more tricyclic terpenes than hopanes are generated from the source rock kerogen due to the greater stability of the former (Aquino-Neto *et al.* 1983). Therefore, the relative amount of C_{23}-C_{29} tricyclic terpanes to C_{30} αβ-hopane (Mello *et al.* 1988; Peters *et al.* 1990; van Graas 1990) has been extensively applied as a good maturity indicator. However, it should be noted that this parameter may have limited applications when used with samples suffering from phase fractionation, evaporative loss and with surface samples from porous rocks (Karlsen *et al.* 2004). Thus, if petroleum is migrated as condensate or gas-phase, this parameter is higher than in the genetically associated oil leg.

Moreover, maturity comparison using this ratio should mainly be done for related oils or source rock extracts, as the tricyclic and hopane compounds have different biological precursors (cf. Peters *et al.* 2005). Ratios for the C_{23}-C_{29} tricyclic terpanes/C_{30} αβ-hopane in this dataset range between 0.36 and 1.34 (Table 3; Fig. 11). It appears that the C_{23}-C_{29} tricyclic/C_{30}αβ-hopane ratio varies significantly among the three sampled sedimentological sections, with values of 0.36–0.49 for the MKW

ACCEPTED MANUSCRIPT

Downloaded from http://pg.lyellcollection.org/ at Universitetet i Oslo on November 21, 2019

section samples, 0.60–0.81 for the NQ section and 0.89–1.34 for the WP92 section, except for WP92-13-14 sample, with the ratio 0.49. While it is clear that the high C_{23}-C_{29} tricyclic/C_{30}αβ-hopane ratios for the WP92 section samples may be due to maturity, in agreement with the above discussion, we interpret this systematic variation to represent mainly phase fractionation and/or organic facies variation (see below).

The sterane/hopane ratio in the sample set, vary from c. 0.23 to nearly 3 , cf. Table 3; Fig. 13, and values in this range is often associated with marine source rock facies for Mesozoic and younger source rocks, with values around 1-3 from typical Jurassic source rock systems. Higher ratios indicate a planktonic source, whilst lower indicate terrigenous material (Tissot & Welte 1984), see Figure 13.

The percentages of regular steranes C_{27}, C_{28} and C_{29}, were calculated from the *m/z*=218 GC-MS chromatograms (Table 3; Fig. 14). Their relative distribution, which largely reflects the original source input, is shown in the ternary diagram of Figure 14. The C_{27}, C_{28} and C_{29} regular steranes for the samples analyzed range from 19 to 35%, 23 to 31% and 36 to 53%, respectively. Values around 33% of C_{29} are very typical for marine source rocks, e.g. the Mesozoic systems, with values towards 50% more typical for terrestrially influenced or coaly source rocks. It is thus clear that the bitumen samples seem all to have been generated from predominantly Type II/III kerogen and with more Type III input for the MKW samples and also the NQ1-7-14 sample (Fig. 14).

The diasteranes (diasteranes + regular steranes) ratio for the samples analyzed varies from 0.22 to 0.46, which indicate immature to early mature maturity window (Table 3; Fig. 11). However, as this ratio will be low in oils from carbonate containing source rocks, interpretation of this parameter for maturity must be based upon supporting parameters (Peters *et al.* 2005).

Aromatic hydrocarbon maturity parameters

Mackenzie *et al.* (1981) reported that during increasing maturity of source rocks more rapid and preferential degradation or conversion of the long-chained (C_{26}-C_{28})

ACCEPTED MANUSCRIPT

Downloaded from http://pg.lyellcollection.org/ at Universitetet i Oslo on November 21, 2019

triaromatic (TA) steroid hydrocarbons over the short chained (C_{20}-C_{22}) homologues is observed. Hence the $C_{20}/(C_{20} + C_{28})$ TA steroid ratio (Fig. 12) will increase with increasing thermal maturity and is applicable throughout the oil window (Mackenzie *et al.* 1981; Peters *et al.* 2005). The $C_{20}/(C_{20} + C_{28})$ TA steroid ratios (Mackenzie *et al.* 1981) for the samples analyzed range between 0.25 and 0.45 (Table 3; Fig. 12), suggesting a maturity range between about 0.6 and 0.8% Rc (Mackenzie *et al.* 1981; Karlsen *et al.* 1995; Peters *et al.* 2005). These results confirm the lower to medium maturity of the samples suggested by the saturated hydrocarbon maturity parameters. Still, as for the tricyclic terpanes this parameter is affected by phase fractionations during migration, which can result in high values, or conversely evaporative loss (Karlsen *et al.* 1995) which will artificially depress the values. Another aromatic maturity parameter, based on the aromatization of the monoaromatic to triaromatic compounds (Mackenzie *et al.* 1985) is the ratio between monoaromatic (MA) and triaromatic steroids (e.g. C_{28} TA/(C_{28} TA + C_{29} MA)). This ratio increases from 0 to unity during thermal maturation (Peters *et al.* 2005), and for the studied samples was found to have values in the range 0.60–0.95 (Table 3; column 17). This parameter, still influenced by phase fractionation, correlates more or less with the $C_{20}/(C_{20} + C_{28})$ TA steroid ratio in that the maturity of the petroleum in the samples lie within early to medium oil window maturity, corresponding to a vitrinite reflectance value of ca. 0.6-0.85% Rc (Karlsen *et al.* 1995; Peters *et al.* 2005).

Medium-range hydrocarbon maturity parameters

The methylphenanthrene ratio, MPR = 2-MP/1-MP, methyl phenanthrene index 1, MPI1 = 1.5 x (3-MP + 2-MP)/(P + 9-MP + 1-MP) and methyl dibenzothiophene ratio, MDR = 4-MDBT/1-MDBT, are all good indicators of maturity (Radke *et al.* 1982; Radke & Welte 1983; Radke *et al.* 1986; Kvalheim *et al.* 1987; Radke 1987, 1988). Maturity assessments, based on these parameters, of oils, condensates and bitumen provide insight into the geochemistry of mixed oils or bitumen blending between *in situ* low maturity bitumen and higher maturity migrated oil (Karlsen *et al.* 1995; Lerch *et al.* 2016b; Abay *et al.* 2017).

Phenanthrene (*m/z* = 178), a C_{14} hydrocarbon compound; methylphenanthrenes (*m/z* = 192), C_{15} compounds and methyldibenzothiophenes (*m/z* = 198), a sulfur

ACCEPTED MANUSCRIPT

Downloaded from http://pg.lyellcollection.org/ at Universitetet i Oslo on November 21, 2019

containing C_{13} compounds were detected by the GC-MS for all investigated samples with strong signal-to-noise ratios. These geomarker compounds are present in oils with concentrations typically 10 to 100 times higher than for the associated biomarkers, and so represent a larger part of the migrating oil. Such compounds are therefore less prone to *in situ* contamination or "pick-up" of low maturity compounds during migration. Consequently, they are very important for maturity assessments (e.g. Karlsen *et al.* 1995; Abay *et al.* 2017). They are also much more abundant in condensates and high GOR systems than in black oils, which is the reason why in-reservoir blending of a condensate with black oil, will result in high geomarker maturities and lower biomarker maturities (cf. Karlsen *et al*. 2004; Karlsen and Skeie 2006).

The MPR, MPI1 and MDR ratios for the sample set are within the range of 0.91–2.00, 0.42–0.86 and 0.45–7.00, respectively (Table 3). This correlates with a vitrinite reflectance between 0.90 and 1.28% Rc calculated from the MPR ratio, 0.65 and 0.92% Rc for the MPI1 ratio and between 0.54 and 1.02% Rc for the MDR ratio (Table 3; Fig. 15).

The MDR ratio can vary between oil and gas prone source rocks, where the former tend to show lower ratios than the latter (Radke *et al.* 1986; Radke 1988). This could suggest that we are dealing with oil-prone source rocks as the MDR seems to be lower than the MPR (metylphenanthrene ratio). It is our general experience that the MDR ratio is more responsive than the MPI1 for oils sourced from Type II/III kerogen, especially at the lower maturity range and at the start of the oil window. Without more detailed knowledge about source rock types than in this study, we would tend to trust more the inferred maturity from MDR than the MPI1, which, however, is usually spot on for coals. The MPI 1 ratio will decrease at a later stage of the oil window, which could be the reason for the lower values we observe compared to the MPR and F1 ratios.

The methylphenanthrene distribution fraction 1 (F1) parameter (Kvalheim *et al.* 1987) is a robust maturity parameter, when phenanthrene (more facies dependent and rich in coals) is excluded in the equation. The F1 values for the samples analyzed range from 0.38 to 0.55 and the corresponding calculated vitrinite reflectance range from 0.69 to 1.07% Rc (Table 3; Fig. 15). Thus, it is clear that most of the samples in this

ACCEPTED MANUSCRIPT

Downloaded from http://pg.lyellcollection.org/ at Universitetet i Oslo on November 21, 2019

dataset contain bitumen generated well within the oil window, including some samples approaching the wet gas window maturity (Fig. 15). According to Figure 15, the samples can be divided into two maturity groups: Group 1, peak oil window maturity; and Group 2, late oil window maturity.

Thus, these parameters suggest that the samples may actually contain petroleum contributions from more than one source rock, or alternatively, the same source rock buried to different maturities.

Age related parameters

The extended tricyclic terpane ratio, ETR = (C_{28} + C_{29})/(C_{28} + C_{29} + Ts) is an age related ratio and applicable to distinguish Jurassic from Triassic samples (Holba *et al.* 2001). Samples from Pre-Triassic sources have also been discerned based on the ETR (Ohm *et al.* 2008). The ETR ratio for the samples analyzed lies between 0.37 and 0.59, which is relatively low and this suggest a Jurassic or younger age (Fig. 16).

The C_{28}/C_{29} ββ steranes ratio increases with a younger geological age (Grantham & Wakefield 1988). This ratio for the studied samples ranges between 0.49 and 0.87, and suggests an age span from the Upper Paleozoic to Cretaceous for the bitumen (Table 3; Fig. 16). However, as seen in Figure 16, it is clear that the C_{28}/C_{29}-sterane ratios are preferentially pointing to the Mesozoic age, most likely Jurassic. Another useful parameter to determine the age of the source rock for oils and bitumen is the C_{26} sterane parameter from the *m/z* = 358 to *m/z* = 217 parent-daughter transition, from which Holba *et al.* (1998) described the nordiacholestane ratio (NDR) as NDR = 24/(24 + 27) nordiacholestanes (Fig. 17). A more recently proposed age parameter is the triaromatic dimethylcholesteroid (TA-DMC) by Barbanti *et al*. (2011) which is useful in distinguishing Paleozoic from Mesozoic aged samples. NDR and TA-DMC ratios are only presented for sample WP92-13-14 and values are 0.22 and 0.16, respectively, suggesting Mesozoic ages (cf. Lerch *et al.* 2018; Matapour & Karlsen 2018).

ACCEPTED MANUSCRIPT

Downloaded from http://pg.lyellcollection.org/ at Universitetet i Oslo on November 21, 2019

Synthesis of the geochemical data – Implications

The distributions of the n-alkanes, isoprenoids, and biomarkers allow for a robust evaluation of the source rock organic facies and for the depositional environment responsible for the source rock that sourced the investigated bitumen. On the logarithmic cross plot of Pr/n-C_{17} vs Ph/n-C_{18} (Fig. 9), a wide range of depositional settings have been inferred: from reducing environments to highly anoxic conditions. According to Figure 9, there is an apparent distinction between the WP92 section samples and the MKW section samples, which are plotted in the highly oxic region of the diagram, where the content of pristane is higher than that of phytane. Samples MKW-1-14 and MKW-5-14 also contain significant amounts of C_{20}+ alkanes with odd-over-even dominance, i.e. a siliciclastic source facies. This suggests that the migrated petroleum in these samples is likely derived from a source rock enriched with Type III kerogen. This interpretation is furthermore substantiated by high C_{29} steranes as well as by the low phytane (Ph) content.

In general, the WP92 section samples suggest a transitional to anoxic source rock setting, with WP92-16-14 and WP92-19-14 being the least terrestrially influenced samples. Minor deviations in these parameters among the samples can also reflect uncertainties due to low signal-to-noise ratio from the GC-FID chromatograms and/or contaminations, which may co-elute with the n-alkanes and isoprenoids (Abay *et al.* 2017). The extremely high Pr/n-C_{17} value for NQ1-1-14 could also be the consequence of such uncertainty. If possible errors are neglected; the n-alkanes and isoprenoid data may suggest coal bearing strata as source rock for the MKW section bitumen. Based on the geological evolution of the Mandawa Basin two major regional petroleum sources most likely rule the Petroleum System: 1) The Permian lacustrine shales from Karoo rifts, and 2) the lower to basal Middle Jurassic shale and marls (Pereira-Rego *et al.* 2013). In terms of age of the source rock for the bitumen, the age specific biomarkers suggest strongly a Mesozoic age for the bitumen and migrated oil, and the Permian system does not seem to be recorded in the bitumen. Why this is the case is unknown at the present time, but it can be that the Permian system is more laterally confined, absent or that, if it at all exists at this location, expelled with an earlier “Critical Moment”. Concerning the organo-facies, the ββ-steranes for most of the samples plot within the estuarine zone, with some lean

ACCEPTED MANUSCRIPT

Downloaded from http://pg.lyellcollection.org/ at Universitetet i Oslo on November 21, 2019

towards a terrestrial input and the MKW-5-14 sample fully within the terrestrial zone (Fig. 14).

The sample set can be divided into three categories based on the geochemical characterization (Fig. 13): 1) MKW-1-14 and MKW-5-14 have the highest values for sterane/hopane and bisnorhopane/(bisnorhopane + norhopane)(BNH), 2) WP92-13-14, WP92-16-14 and WP92-19-14 have fairly high sterane/hopane ratios (range: 1.28–2.66), but low bisnorhopane/(bisnorhopane + norhopane), 3) The three samples WP92-5-14, WP92-7-14 and WP92-11-14 have low ratios for both the parameters.

Higher BNH abundance is reflecting anoxic marine conditions, but meager quantities of BNH do not necessarily exclude anoxia (Peters *et al.* 2005). It is, furthermore, crucial to note from this that there is a systematic variation in geochemical parameters between the WP92 section samples, which constitute Upper Jurassic and Lower Cretaceous parts of the Kipatimu Formation), cf. Figure 13.

As an example of this, the presented sterane/hopane and BNH ratios for the WP92-5-14, WP92-7-14 and the WP92-11-14 (samples from the Upper Jurassic part of the WP92 section) range from 0.23 to 0.38 and from 0.06 to 0.08, respectively, while that of the WP92-19-14, the WP92-16-14 and WP92-13-14 (samples from the Lower Cretaceous of the section) range from 1.28 to 2.66 and from 0.09 to 0.25, respectively. Higher relative amounts of steranes than bacterial hopanoids is generally a feature of marine depositional environment (Peters *et al.* 2005) or high organic productivity (Volkman 1988). We suggest that this interpretation is reliable as the sterane/hopane ratio is significantly maturity independent until the later part of the oil-window when steranes tend to dominate over hopanes due to their smaller molecular size and hence higher thermal stability (Karlsen *et al.* 2004). During thermal maturation, bisnorhopane will degrade, so the discrepancies could also reflect different maturities (Curiale *et al.* 1985).

Summary of Maturity

Organic geochemical maturity parameters indicate that the Mandawa Basin bitumen samples represent early to peak oil window expulsion maturities. However, there is great variability in the maturity of the samples from section to section and within the

ACCEPTED MANUSCRIPT

Downloaded from http://pg.lyellcollection.org/ at Universitetet i Oslo on November 21, 2019

sections. Such variation will normally reflect different and separate pulses of migration, including potential remigration from deeper traps.

As example of the variation, consider the Ts/(Ts + Tm) and diasterane/(diasterane + regular steranes) ratio which generally expresses a low maturity for the samples, from immature to early oil window generation. WP92-13-14, NQ1-1-14 and MKW-1-14 deviate slightly from the rest of the sample set with higher maturities (Fig. 11). Still a low ratio can very well be due to original source input, indicating a carbonate heritage.

Based on the 29Ts/(29Ts + norhopane) ratio two distinct maturity families can be discerned. The MKW and NQ samples from the southern and central part, respectively, of the Mandawa Basin have a higher maturity than the WP92 samples from the northern part (Figs 10 and 11). The 29Ts/(29Ts + norhopane) is less influenced by source input compared to other saturated hydrocarbon maturity parameters, and consequently represents one of the most robust maturity parameters (Karlsen & Skeie 2006).

Based on Figure 12 most of the samples appear to fall within the early-peak oil generation window. Sample WP92-5-14, WP92-7-14 and WP92-16-14 display a low maturity based $C_{20}/(C_{20} + C_{28})$ TA steroid ratios. However, the C_{23}-C_{29} tricyclic terpane ratios for the same samples estimate a higher maturity than the rest of the sample set. This could be due to phase fractionation during migration, where the samples WP92-5-14, WP92-7-14 and WP92-16-14 trapped parts of a lighter fraction. The lighter part (higher API and GOR) of isolated oil has a tendency to become enriched in C_{23}-C_{29} tricyclic terpanes and C_{20} triaromatic steroids, while the heavier oil fraction (the oil-leg) will have higher abundances of $C_{30}\alpha\beta$ hopane and C_{28} triaromatic steroid. This is due to the lower molecular weight of C_{23}-C_{29} tricyclic terpanes and C_{20} triaromatic steroid (Karlsen *et al.* 1995; Karlsen & Skeie 2006). Separation of the phases occurs because of PVT changes throughout migration (England & Mackenzie 1989) and is likely in this setting with fault induced dismigration in relation to uplift/tilting and tectonism. In such faults, PVT-associated phase fractionation is likely (Karlsen & Skeie 2006). The sample set appears to have a higher maturity based on the diahopane/(diahopane + normoretan) ratio. This can be due to the influence of a terrigenous source input. Diahopane stems from

ACCEPTED MANUSCRIPT

Downloaded from http://pg.lyellcollection.org/ at Universitetet i Oslo on November 21, 2019

hopanes via isomeric reorganized by a clay-mediated catalyst in an oxic- to sub-oxic terrigenous environment (Peters *et al.* 2005). This concurs with the observation of Volkman *et al.* (1983), Alexander *et al.* (1983) and Philp & Gilbert (1986) where diahopane is found in large quantities in terrigenous oils. The samples WP92-5-14, MKW-5-14 and NQ1-1-14 display some of the highest maturities in terms of the diahopane/(diahopane + normoretane) ratio correlating well with the C_{27}, C_{28} and C_{29} sterane plots, where the respective samples seem to be influenced by terrigenous input (Fig. 14).

Hydrocarbon migration and age determination of the source rocks

The presence of n-alkanes from n-C_{15} to n-C_{35} in sample WP92-13-14 and MKW-5-14 (Fig. 8) witness generation of oil in a deeply buried source rock, and migration of petroleum into the investigated formations, and this matches well the maturity plots which also predicts the presence of petroleum within the oil window. Our maturity estimates based upon geomarkers and biomarkers confirm that the bulk of the bitumen samples were generated at maturities between early-, to peak oil-window maturities suggesting that a number of the samples contain blended hydrocarbon signatures from one or more source rocks, or the same source rock expelling at highly different maturities. Alternatively, the bitumen can also represent several re-migration episodes related to uplift and structural readjustments which seem to be likely as most samples occur close to faults/fracture systems.

Based on the PI we can classify six of the samples analyzed as irrefutably migrated petroleum; MKW-1-14, NQ1-7-14, WP92-5-14, WP92-13-14 and WP92-7-14, WP92-16-14 (Fig. 7). This coincides well with the n-alkanes present in the WP92-13-14 sample (Fig. 8). Samples NQ1-1-14, WP92-19-14, MKW-5-14 and WP92-11-14 with a PI slightly less than 0.4 could also stem from migrated petroleum, but possibly with a slight *in situ* contribution from kerogen, or more likely a heavy S2 contribution from biodegraded oil and bitumen. Asphaltene content of this nature will not contribute to the S1 signal, but to the S2 signal and contribute to a depressed PI value. For the remaining samples (i.e. NQ1-3-14, NQ2-2-14 and HTQ1-14, see Table 2) the PI values are low, and indicate *in situ* bitumen, and/or biodegraded oil/bitumen.

ACCEPTED MANUSCRIPT

Downloaded from http://pg.lyellcollection.org/ at Universitetet i Oslo on November 21, 2019

The accepted upper PI limit for a source rock at the end of the oil window is less than 0.40 (Hunt 1996; Abay *et al.* 2018). None of the samples appears to have good source rock qualities based on the TOC, where the highest one is assigned to NQ1-3-14 with 1.13 wt%. Thus, it is likely that biodegraded bitumen in the form of asphaltenes has contributed to the already low S2 signal of the samples. Moreover, the Hydrogen Index (HI: an expression of hydrocarbon yield which takes into account of the TOC and S2 Rock-Eval) is very low for the samples to be potential source rocks.

Complications due to oxidized OM and biodegraded bitumen/oil was anticipated given that the samples analyzed originate from outcrops in a tropical climate. The presence of unresolved complex mixture (UCM) in WP92-13-14, and MKW-5-14 samples (Fig. 8) reflects several episodes of biodegradation following intermittent replenishment by fresh oil (Duncan & Hamilton 1988; Abay *et al.* 2014, 2017), which was already or at a later stage biodegraded by microbial activity. The GC-FID chromatograms of these samples contain n-alkanes up to n-C_{30+} i.e. black-oil proper, in a heavy hydrocarbon fraction, while the lighter n-alkanes are mostly absent probably because of biodegradation and evaporation. Moreover, quite similar GC-FID chromatograms can be seen from the SongoSongo-5 with a waxy appearance, showing n-alkanes from n-C_{15} to n-C_{30} and similar n-alkane patterns as observed in WP92-13-14 (Pereira-Rego *et al.* 2013). Biodegradation can also be inferred from the UCM in the chromatograms of the SongoSongo-5 sample (Pereira-Rego *et al.* 2013). The C_{29} norhopane peak is smaller than the C_{30} hopane for the SongoSongo sample which is also true for the sample set in this paper.

A possible source rock in the Mandawa Basin is the Upper Triassic to Lower Jurassic evaporitic-shale sequence of the Nondwa Formation (Kagya 1996). However, only one sample WP92-16-14 contains a small amount of gammacerane, a key biomarker indicative of high salinity depositional environments, which Kagya (1996) noted in samples from the Nondwa (Pindiro Evaporite) Formation (Moldowan *et al.* 1985; Peters *et al.* 2005).

The geological communication between sample sites of WP92 (northern Mandawa), NQ (central Mandawa) and MKW (southern Mandawa) may have been restricted if the E-W oriented fault planes have been sealing. This most likely could have blocked

ACCEPTED MANUSCRIPT

Downloaded from http://pg.lyellcollection.org/ at Universitetet i Oslo on November 21, 2019

migration in an N-S direction. However, the geochemical signatures appears quite similar in all the samples, which could reflect petroleum migration coming from the west or east and possibly at an earlier stage, before the severe tectonic movements. A possible migration route could be towards the west since the subsidence of the sediments has been greater in east.

The extended tricyclic terpane ratios (ETR, Fig. 16) are often found to be a good indicator to distinguish the boundary between Triassic and Jurassic, a notion possibly related to the mass extinction in Late Triassic, which is believed to have had an influence on the source of tricyclic terpanes such as Tasmanites (Peters *et al.* 2005). Moreover, a later extinction during the Toarcian, may also make it possible to separate Early Jurassic sources from Middle and Late Jurassic (Holba *et al.* 2001). The ETR ratios for the samples are all below 0.6 and within a narrow range (Fig. 16). Consequently, the ETR could suggest Middle to Late Jurassic age for the entire sample set. The ratio of C_{28}/C_{29} ββ steranes coincide with ETR, indicating a Jurassic source, albeit, not Upper Jurassic.

The bitumen samples are thus suggested to be, in terms of source rock age related to the Lower Jurassic, with the only samples that deviate being NQ1-1-14 and WP92-13-14, which are estimated to be of Upper Jurassic and possibly Cretaceous or younger, respectively (Fig. 16).

To further narrow down the source rock age, the ratio of 24- to 27-nordiacholestanes (NDR) were investigated. The 24-nordiacholestanes are biomarkers of diatoms and dinoflagellates (Rampen *et al.* 2007), which increases in abundance with decreasing age, reflecting the phylogenetic radiation of the parent organisms (Fig. 17). A ratio exceeding 0.2 is an indication of Jurassic or younger sources. The WP92-13-14 sample has NDR ratio of 0.22, which indicates a Jurassic source, harmonizing well with the other age determination ratios (Fig. 16).

Independent data, supporting a Mesozoic and possible Jurassic age for the bitumen, is the triaromatic 23,24-dimethylcholesteroids ratio (TA-DMC), cf. Barbanti *et al.* (2011), Matapour & Karlsen (2018) and Lerch *et al.* (2018). The absence of these triaromatic dimethylcholesteroids would support a Paleozoic source, while the presence is consistent with a Mesozoic age (Barbanti *et al.* 2011), although some

ACCEPTED MANUSCRIPT

Downloaded from http://pg.lyellcollection.org/ at Universitetet i Oslo on November 21, 2019

Late Permian sources have shown similar or higher ratios than the Lower Triassic source rocks (Lerch *et al.* 2018). This offers an independent method to confirm the source age. The TA-DMC ratio for the WP92-13-14 bitumen was estimated to be 0.16, a value strongly suggesting a source rock younger than the Paleozoic (Fig. 17).

Conclusions

- The samples analyzed show that the potential Mandawa Basin reservoir rocks contain both migrated petroleum from mature source rocks and a minor contribution of locally derived hydrocarbons, comparable to the SongoSongo petroleum system.
- Migrated hydrocarbon compounds of the migrated bitumen have been recognized in all three sections investigated, with likely migration from the east to the west.
- The migrated petroleum was generated from a source rock containing Type II/III kerogen most likely deposited in estuarine to open marine environments.
- Several stages of migration and remigration into the sampled locations are likely as there is evidence for repeated and variable degrees of biodegradation in the form of significant UCMs, coexisting with a series of n-alkanes and conflicting maturity signatures in the bitumen. This probably reflects intermittent leakage and remigration from deeper pools during late uplift and tectonic readjustments.
- The source rock for the migrated bitumen is, based on age-specific biomarkers and general facies signatures, likely to reside within the Karoo sequence, or more specifically the Lower Jurassic formation in coastal areas of the Mandawa Basin.
- Implications of the study include that oil-window mature source rocks exist in the study region, with possible implications to the offshore basins. Thus, the inferred “Petroleum System” should contain oil-generative source rocks.
- Further evaluations of oil-seeps and migrated bitumen from the general region should be compared to offshore samples of gas, condensates and oil in order

ACCEPTED MANUSCRIPT

Downloaded from http://pg.lyellcollection.org/ at Universitetet i Oslo on November 21, 2019

to better constrain the migration regime/style of the Mandawa petroleum system.

- As a corollary we note that the Inhassoro, Pande and Temane gas systems, offshore Mozambique, are reinterpreted to be oil-window mature, oil-associated and not over-mature as previously suggested. Rather, severe phase separation during vertical migration is the likely cause of the high API petroleum systems observed, with the potential for oil deeper down-dip.
- We conclude on this basis that there is a definite need for an integrated cross-border “Petroleum System” re-evaluation of all gases, oil-seeps and condensates from offshore Mozambique and Tanzania.
- Future geochemical studies using shallow coring over the basin and satellite imageries are recommended.

Acknowledgements

We thank N. H. Hanken, A. Read and others for helpful comments and discussions. The authors thank T. Naidoo, S. Akhavan and K. Backer-Owe at the Geochemical Laboratories of the Department for Geosciences, University of Oslo, for technical support. Thanks are also due to Majkel van der Brink, CGuanqun Hou, Didas Makoye, Alexandra Cournot and Amina Karega for their participation during the field work.

We thank Equinor (formerly Statoil) for financial support.

ACCEPTED MANUSCRIPT

Downloaded from http://pg.lyellcollection.org/ at Universitetet i Oslo on November 21, 2019

Figure captions:

Fig. 1. Map of southern coastal Tanzania and northern costal Mozambique with the recent gas discoveries and surface oil seeps highlighted. Note the occurrence of seeps in possible causal relation to the faults indicating significant vertical migration. Modified from Davison and Steel (2018).

Fig. 2. Geological map of the Mandawa Basin showing sample locations. Modified from Hudson (2011) and Fossum et al. (2018).

Fig. 3. Stratigraphical chart for the Mandawa Basin. Modified from Hudson (2011) and Fossum et al. (2018).

Fig. 4. Sedimentological logs of the studied sections with sample beds marked.

Fig. 5. (**a**) Location map of onshore Mozambique gas fields (Pande, Temane and Inhassoro fields), from Loegering & Milkov (2017). (b) Comparison of gas data from onshore fiends of Mozambique (Pande, Temane and Inhassoro fields) with Norwegian North Sea and Norwegian Sea gases. The iso-butane to normal-butane (i-C4/n-C4) ratio increases with biodegradation, and a value of around 0.45–0.55 is typical for non-biodegraded thermogenic hydrocarbon gas systems, and higher values are in Norway associated with biodegraded gases form shallow strata. Thus, the Mozambique gas data are severely biodegraded, contrary to the conclusion of Loegering & Milkov (2017). Note that several of the Norwegian Sea gas data are from structurally uplifted traps, where gases are biodegraded, while the North Sea gases are mostly occurring in traps with a simpler and more direct charge-style, and the butane ratios are accordingly lower.

Fig. 6. Field photo and thin section representing the MKW-5-14 sample.

Fig. 7. Cross-plot of production index (PI) versus total organic carbon (TOC). PI values higher than 0.40 normally indicates migrated petroleum (Hunt, 1996). Sample MKW-1-14 shows the strongest evidence of migrated petroleum followed by WP92-7-14, WP92-13-14, NQ1-7-14, WP92-5-14 and WP92-16-14. The remaining samples have PI values in line with *in situ* generated petroleum. In addition other outcrop samples from the Mandawa Basin analyzed by Hudson (2011) have been included for comparison. The Hudson (2011) data points imply both migrated and *in situ* generated petroleum.

Fig. 8. GC-FID chromatograms of samples WP92-13-14 and MKW-5-14. Normal alkanes and isoprenoids are indicated (e.g. n-C_{17} = n-heptadecane; n-C_{18} = n-octadecane; Pr = pristane; Ph = phytane), and have been identified in both chromatograms. Some uncertainty exist for the later sample in the lower alkane group (<C_{20}), due to unidentified peaks with higher signal than the n-alkanes and isoprenoids. These peaks are partly unidentified contaminants. UCM = unresolved complex mixture, see text.

ACCEPTED MANUSCRIPT

Downloaded from http://pg.lyellcollection.org/ at Universitetet i Oslo on November 21, 2019

Fig. 9. Plot of pristane/n-C_{17} versus phytane/n-C_{18} illustrating organic facies variation, maturation and biodegradation (after Shanmugam, 1985). The analyzed samples display a wide spread in these parameters, possibly reflecting more than one source rock facies, varying from marine to terrestrial. Samples NQ1-1-14, MKW-1-14, and MKW-5-14 display extremely high values of Pr/n-C_{17} likely caused by biodegradation of these surface samples, and/or contamination which coelutes with C_{17} n-alkane in the GC-FID chromatogram.

Fig. 10. Ion chromatogram of m/z = 191 of the tricyclic terpane, hopane and homohopane peaks of samples WP92-13-14 and MKW-5-14. Peak identification followed Abay *et al*. (2014).The values for calculated parameters for these peaks occur in Table 3.

Fig. 11. Cross-plots of maturity parameters suggesting low maturity to early oil window maturity. (A) The cross plot of Ts/ (Ts + Tm) versus diasteranes/ (diasteranes + regular steranes) implies low maturity of the samples (after Seifert and Moldowan, 1978). Due to low signal-to-noise ratio of sample NQ1-7-14, the diasteranes/ (diasterane + regular sterane) ratio was not calculated. (B) Plot of Ts/ (Ts + Tm) versus 29Ts/ (29 Ts + norhopane).

Fig. 12. The maturity of the samples based on saturated and aromatic biomarkers. (**a**) Plot of $C_{20}/(C_{20} + C_{28})$ versus C_{23}-C_{29} tricyclic terpanes/C_{30} aβ hopane. (**b**) $C_{20}/(C_{20} + C_{28})$ versus diahopane/ (diahopane + normoretane). Note that the order of maturity of the samples is inverted when plotted in the two diagrams which suggest that the samples have been subjected to evaporation and/or phase fractionation during migration.

Fig. 13. Cross plot of sterane/hopane (Tissot & Welte 1984) versus bisnorhopane/(bisnorhopane + norhopane) (Wilhelms & Larter 1994). The samples appear to be heavily influenced by terrestrial input. Still, the MKW-1-14 and MKW-5-14 samples are skewed towards marine source composition.

Fig. 14. Ternary diagram illustrating variations in depositional environment of the source rocks based on the distribution of C_{27}, C_{28} and C_{29} regular steranes (after Shanmugam 1985). All samples plot in the estuarine area, except for sample MKW5-14 which plots in the terrestrial area of the diagram.

Fig. 15. Cross-plots of calculated vitrinite reflectance displaying the variation in maturity of the samples based on aromatic compounds. (**a**) %Rm = 0.073 x MDR + 0.51 (Radke 1988) versus %Rc = 0.60 x MPI 1 + 0.40 (Radke & Welte 1983). (**b**) Rm = 1.1 x $\log_{10}$ MPR + 0.95 (Radke, 1988) versus %Ro = 2.242*F1 - 0.166 (Kvalheim *et al*. 1987) (where MDR: methyldibenzothiophene ratio (Radke, 1988); MPI 1: methylphenanthrene index I (Radke *et al*. 1982); MPR: methylphenanthrene ratio (Radke 1988); F1: methylphenanthrene distribution fraction (Kvalheim *et al.* 1987). Note that the maturity level of these geomarkers appears to be different than what

ACCEPTED MANUSCRIPT

Downloaded from http://pg.lyellcollection.org/ at Universitetet i Oslo on November 21, 2019

was observed for the biomarkers, something often observed in multi-stage migrated bitumen.

Fig. 16. Age determination of bitumen and the inferred source rock based on the C_{28}/C_{29} ββ sterane ratios and extended tricyclic terpane ratio (ETR). The sample spread implies the possibility of three petroleum groups in the analyzed samples with the majority of the samples being derived from Upper Paleozoic to Lower Jurassic source rocks.

Fig. 17. GC-MS/MS chromatograms of 24- and 27- nordiacholestane (m/z 358 → 217) and of triaromatic dimenthylcholesteroid (m/z 372 → 231) for sample WP92-13-14. Nordiacholestane ratio (NDR; Holba *et al*. 1988) and triaromatic dimethylcholesteroid (TA-DMC: Barbanti *et al*. 2011) ratio of 0.22 and 0.16, respectively suggest irrefutably Mesozoic age source rocks for the migrated petroleum in sample WP92-13-14.

Tables:

Table 1. *Sample overview.*

Table 2. *TOC and Rock-Eval data.*

Table 3. *Maturity and facies parameters calculated from GC-FID and GC-MS chromatograms.*

ACCEPTED MANUSCRIPT

Downloaded from http://pg.lyellcollection.org/ at Universitetet i Oslo on November 21, 2019

References

Abay, T.B., Karlsen, D.A. & Ohm, S. 2014. Vertical variations in reservoir geochemistry in a palaeozoic trap, Embla field, offshore Norway. *Journal of Petroleum Geology*, **37**, 349-372, http://doi.org/10.1111/jpg.12590.

Abay, T.B., Karlsen, D.A., Lerch, B., Olaussen, S., Pedersen, J.H. & Backer‐Owe, K. 2017. Migrated petroleum in outcropping Mesozoic sedimentary rocks in Spitsbergen: Organic geochemical characterization and implications for regional exploration. *Journal of Petroleum Geology*, **40**, 5-36, http://doi.org/10.1111/jpg.12662.

Abay, T.B., Karlsen, D.A., Pedersen, J.H., Olaussen, S. & Backer-Owe, K. 2018. Thermal maturity, hydrocarbon potential and kerogen type of some Triassic–Lower Cretaceous sediments from the SW Barents Sea and Svalbard. *Petroleum Geoscience*, **24**, 349-373, http://doi.org/10.1144/petgeo2017-035.

Aitken, W. 1961. The geology and palaeontology of the Jurassic and Cretaceous of southern Tanganyika. *Bulletin of the Geological Survey of Tanganyika*, **31**, 1-144.

Alexander, R., Kagi, R.I., Woodhouse, G.W. & Volkman, J.K. 1983. The geochemistry of some biodegraded Australian oils. *Australian Petroleum Exploration Association Journal*, **23**, 53-63.

Aquino-Neto, F.R., Trendel, J.M., Restle, A., Connan, J. & Albrecht, P.A. 1983. Occurrence and Formation of Tricyclic and Tetracyclic Terpanes in Sediments and Petroleums. *In*: M. Bjorøy, C. Albrecht, C. Cornford, K. de Groot, G. Eglington, E. Galimov, D. Leythaeuser*, et al.* (eds) *Advances in Organic Geochemistry 1981, Wiley, Chichester (1983)*, 659-667.

Barbanti, S.M., Moldowan, J.M., Watt, D.S. & Kolaczkowska, E. 2011. New triaromatic steroids distinguish Paleozoic from Mesozoic oil. *Organic Geochemistry*, **42**, 409-424.

Barlass, D., Zibane, M., Samuel, C., Langa, H. & Tembe, C. 2017. Prospectivity Analysis and Resource Assessment of the Unlicensed Angoche Basin. Abstarct presented at the *Third EAGE Eastern Africa Petroleum Geoscience Forum,* http://doi.org/10.3997/2214-4609.201702396.

Boote, D.R.D. & Matchette-Downes, C. 2009. Extinct and near extinct petroleum systems of the East African coastal basins. Presented at the 8th PESGB/HGS Conference on African E & P. Queen Elizabeth II Conference Centre, 9–10 September 2009, London.

Bosellini, A. 1992. The Continental Margins of Somalia: Structural Evolution and Sequence Stratigraphy. *American Association of Petroleum Geologists. Memoir*, **53**, 185–205.

ACCEPTED MANUSCRIPT

Downloaded from http://pg.lyellcollection.org/ at Universitetet i Oslo on November 21, 2019

Cornford, C., Needham, C. & De Walque, L. 1986. Geochemical habitat of North Sea oils and gases. *In*: Spencer, A.M. (ed) *Habitat of hydrocarbons on the Norwegian continental shelf*. Graham and Trotman, London, 39-54.

Curiale, J.A., Cameron, D. & Davis, D.V. 1985. Biological marker distribution and significance in oils and rocks of the Monterey Formation, California. *Geochimica et Cosmochimica Acta*, **49**, 271-288.

Davison, I. & Steel, I. 2018. Geology and hydrocarbon potential of the East African continental margin: a review. *Petroleum Geoscience*, **24**, 57-91, http://doi.org/10.1144/petgeo2017-028.

Didyk, B., Simoneit, B., Brassell, S.t. & Eglinton, G. 1978. Organic geochemical indicators of palaeoenvironmental conditions of sedimentation. *Nature*, **272**, 216-222.

Duncan, A. & Hamilton, R. 1988. Palaeolimnology and organic geochemistry of the Middle Devonian in the Orcadian Basin. *Geological Society, London, Special Publications*, **40**, 173-201.

Eagles, G. & König, M. 2008. A model of plate kinematics in Gondwana breakup. *Geophysical Journal International*, **173**, 703-717.

England, W.A. & Mackenzie, A.S. 1989. Some aspects of the organic geochemistry of petroleum fluids. *Geologische Rundschau*, **78**, 291-303.

Fossum, K., Morton, A.C., Dypvik, H. & Hudson, W.E. 2018. Integrated heavy mineral study of Jurassic to Paleogene sandstones in the Mandawa Basin, Tanzania: Sediment provenance and source-to-sink relations. *Journal of African Earth Sciences*, **In press**, http://doi.org/10.1016/j.jafrearsci.2018.09.009.

Galimov, E. M., 1973. Carbon isotopes in oil and gas geology (In Russian). *Moscow, Nedra, English translation, Washington, NASA TT F-682, Washington, D.C., 1975*, 384 pp.

Galimov, E. M., 1985. The biological fractionation of isotopes. Academic Press, Inc., Orlando, 261.

Gaina, C., Torsvik, T.H., van Hinsbergen, D.J., Medvedev, S., Werner, S.C. & Labails, C. 2013. The African Plate: A history of oceanic crust accretion and subduction since the Jurassic. *Tectonophysics*, **604**, 4-25.

Geiger, M., Clark, D.N. & Mette, W. 2004. Reappraisal of the timing of the breakup of Gondwana based on sedimentological and seismic evidence from the Morondava Basin, Madagascar. *Journal of African Earth Sciences*, **38**, 363-381.

Grantham, P.J. & Wakefield, L.L. 1988. Variations in the sterane carbon number distributions of marine source rock derived crude oils through geological time. *Organic Geochemistry*, **12**, 61-73, http://doi.org/10.1016/0146-6380(88)90115-5.

ACCEPTED MANUSCRIPT

Downloaded from http://pg.lyellcollection.org/ at Universitetet i Oslo on November 21, 2019

Gundersveen, E. 2014. *Sedimentology, Petrology and Diagenesis of Mesozoic Sandstones in the Mandawa Basin, Coastal Tanzania.* M. Sc. thesis, University of Oslo, 105 pp.

Gussow, W.C. 1954. Differential entrapment of oil and gas: a fundamental principle. *AAPG bulletin*, **38**, 816-853.

Haid, M.H.M. 2018. *Depositional Environments of the Lower Cretaceous Nalwehe Formation of Mandawa Basin, Southern Coastal Tanzania. A study based on mineralogical-and petrographical analysis.* M. Sc. thesis, University of Oslo, 127 pp.

Holba, A., Tegelaar, E., Huizinga, B., Moldowan, J., Singletary, M., McCaffrey, M. & Dzou, L. 1998. 24-norcholestanes as age-sensitive molecular fossils. *Geology*, **26**, 783-786.

Holba, A., Ellis, L., Dzou, L., Hallam, A., Masterson, W., Francu, J. & Fincannon, A. 2001. *Extended tricyclic terpanes as age discriminators between Triassic, Early Jurassic and Middle-Late Jurassic oils (abs.): 20th International Meeting on Organic Geochemistry, 10-14 September, 2001, Nancy, France, v. 1, 464 pp*.

Hudson, W.E. 2011. *The geological evolution of the petroleum prospective Mandawa Basin southern coastal Tanzania.* PhD thesis, Trinity College, University of Dublin, Ireland, 357 pp.

Hudson, W.E. & Nicholas, C.J. 2014. The Pindiro Group (Triassic to Early Jurassic Mandawa Basin, southern coastal Tanzania): Definition, palaeoenvironment, and stratigraphy. *Journal of African Earth Sciences*, **92**, 55-67.

Hunt, J.M. 1996. *Petroleum Geochemistry and Geology, 2nd Edition*. 2nd. ed. W.H. Freeman and Company, New York.

Kagya, M.L.N. 1996. Geochemical characterization of Triassic petroleum source rock in the Mandawa basin, Tanzania. *Journal of African Earth Sciences*, **23**, 73-88.

Kapilima, S. 2003. Tectonic and sedimentary evolution of the coastal basin of Tanzania during the Mesozoic times. *Tanzania Journal of Science*, **29**, 1-16.

Karlsen, D.A. & Larter, S. 1989. A rapid correlation method for petroleum population mapping within individual petroleum reservoirs: applications to petroleum reservoir description. *In*: Collinson, J.D. (ed) *Correlation in Hydrocarbon Exploration*. Springer Netherlands, 77-85.

Karlsen, D.A. & Larter, S.R. 1991. Analysis of petroleum fractions by TLC-FID: applications to petroleum reservoir description. *Organic Geochemistry*, **17**, 603-617.

Karlsen, D.A., Nedkvitne, T., Larter, S.R. & Bjørlykke, K. 1993. Hydrocarbon composition of authigenic inclusions: application to elucidation of petroleum reservoir filling history. *Geochimica et Cosmochimica Acta*, **57**, 3641-3659.

ACCEPTED MANUSCRIPT

Downloaded from http://pg.lyellcollection.org/ at Universitetet i Oslo on November 21, 2019

Karlsen, D.A. & Skeie, J.E. 2006. PETROLEUM MIGRATION, FAULTS AND OVERPRESSURE, PART I: CALIBRATING BASIN MODELLING USING PETROLEUM IN TRAPS — A REVIEW. *Journal of Petroleum Geology*, **29**, 227-256, http://doi.org/10.1111/j.1747-5457.2006.00227.x.

Karlsen, D.A., Nyland, B., Flood, B., Ohm, S.E., Brekke, T., Olsen, S. & Backer-Owe, K. 1995. Petroleum geochemistry of the Haltenbanken, Norwegian continental shelf. *Geological Society Special Publications*, **86**, 203-256.

Karlsen, D.A., Skeie, J.E., Backer-Owe, K., Bjørlykke, K., Olstad, R., Berge, K., Cecchi, M., Vik, E., *et al.* 2004. Petroleum migration, faults and overpressure. Part II. Case history: the Haltenbanken Petroleum Province, offshore Norway. *Geological Society, London, Special Publications*, **237**, 305-372.

Kent, P.E., Hunt, J.A. & Johnstone, D.W. 1971. The geology and geophysics of coastal Tanzania. *Institute of Geological Sciences, Geophysical Papers*, **6**, 1-101.

Kvalheim, O.M., Christy, A.A., Telnæs, N. & Bjørseth, A. 1987. Maturity determination of organic matter in coals using the methylphenanthrene distribution. *Geochimica et Cosmochimica Acta*, **51**, 1883-1888, http://doi.org/10.1016/0016-7037(87)90179-7.

Lerch, B., Karlsen, D.A., Abay, T.B., Duggan, D., Seland, R. & Backer-Owe, K. 2016a. Regional petroleum alteration trends in Barents Sea oils and condensates as a clue to migration regimes and processes. *AAPG bulletin*, **100**, 165-190, http://doi.org/10.1306/08101514152.

Lerch, B., Karlsen, D.A., Matapour, Z., Seland, R. & Backer-Owe, K. 2016b. Organic geochemistry of Barents Sea petroleum: thermal maturity and alteration and mixing processes in oils and condensates. *Journal of Petroleum Geology*, **39**, 125-148, http://doi.org/10.1111/jpg.12637.

Lerch, B., Karlsen, D.A., Thießen, O., Abay, T.B., van Soelen, E.E., Kürschner, W.M., Planke, S. & Backer-Owe, K. 2018. Investigations on the use of triaromatic dimethylcholesteroids as age-specific biomarkers in bitumens and oils from Arctic Norway. *Organic Geochemistry*, **122**, 1-16, http://doi.org/10.1016/j.orggeochem.2018.04.011.

Loegering, M.J. & Milkov, A.V. 2017. Geochemistry of petroleum gases and liquids from the Inhassoro, Pande and Temane Fields Onshore Mozambique. *Geosciences*, **7**, 33, http://doi.org/10.3390/geosciences7020033

Mackenzie, A., Patience, R., Maxwell, J., Vandenbroucke, M. & Durand, B. 1980. Molecular parameters of maturation in the Toarcian shales, Paris Basin, France—I. Changes in the configurations of acyclic isoprenoid alkanes, steranes and triterpanes. *Geochimica et Cosmochimica Acta*, **44**, 1709-1721.

Mackenzie, A.S., Hoffmann, C.F. & Maxwell, J.R. 1981. Molecular parameters of maturation in the Toarcian shales, Paris Basin, France – III. Changes in aromatic steroid hydrocarbons. *Geochimica et Cosmochimica Acta*, **45**, 1345-1355.

Mackenzie, A. S., Maxwell, J. R., Coleman, M. L. & Deegan, C. E. 1984. Biological marker and carbon isotope studies of North Sea crude oils and sediments. In: Proceedings of the 11th Worm Petroleum Congress, Vol. 2. John Wiley & Sons, Chichester,45-56.

ACCEPTED MANUSCRIPT

Downloaded from http://pg.lyellcollection.org/ at Universitetet i Oslo on November 21, 2019

Mackenzie, A.S., Beaumont, C., Boutilier, R. & Rullkötter, J. 1985. The aromatization and isomerization of hydro carbons and the thermal and subsidence history of the Nova Scotia margin. *Phil. Trans. R. Soc. Lond. Series A*, **315**, 203-232.

Mahanjane, E., Franke, D., Lutz, R., Winsemann, J., Ehrhardt, A., Berglar, K. & Reichert, C. 2014. Maturity and petroleum systems modelling in the offshore Zambezi Delta depression and Angoche Basin, northern Mozambique. *Journal of Petroleum Geology*, **37**, 329-348.

Makoye, D.M. 2016. *Geophysicalinvestigation of the subsurface structures of the Mandawa Basin, Southeast Coastal Tanzania. M.Sc thesis, Univ. of Dar es Salaam, 155pp.*

Matapour, Z. & Karlsen, D. 2018. Ages of Norwegian oils and bitumen based on age-specific biomarkers. *Petroleum Geoscience*, **24**, 92-101.

Mbede, E.I. 1991. The sedimentary basins of Tanzania-reviewed. *Journal of African Earth Sciences (and the Middle East)*, **13**, 291-297.

McKirdy, D., Aldridge, A. & Ypma, P. 1983. A geochemical comparison of some crude oils from pre-Ordovician carbonate rocks *Advances in Organic Geochemistry 1981*. Wiley Chichester, 99-107.

Mello, M., Gaglianone, P., Brassell, S. & Maxwell, J. 1988. Geochemical and biological marker assessment of depositional environments using Brazilian offshore oils. *Marine and Petroleum Geology*, **5**, 205-223.

Mkuu, D.E. 2018. *Palynological, palynofacies, thermal maturity and burial modelling analyses of the Cretaceous to Cenozoic sediments from a series of Tanzanian onshore and offshore boreholes.* PhD thesis, University of Southampton.

Moldowan, J.M., Seifert, W.K. & Gallegos, E.J. 1985. Relationship between petroleum composition and depositional environment of petroleum source rocks. *AAPG bulletin*, **69**, 1255-1268.

Moldowan, J.M., Fago, F.J., Carlson, R.M.K., Young, D.C., Van Duyne, G., Clardy, J., Schoell, M., Pillinger, C.T., *et al.* 1991. Rearranged hopanes in sediments and petroleum. *Geochimica et Cosmochimica Acta*, **55**, 3333-3353.

Mpanda, S. 1997. *Geological development of the East African coastal basin of Tanzania.* Acta Universitatis Stockholmiensis.

Mpanju, F. & Philp, R. 1994. Organic geochemical characterization of bitumens, seeps, rock extracts and condensates from Tanzania. *Organic Geochemistry*, **21**, 359-371.

ACCEPTED MANUSCRIPT

Downloaded from http://pg.lyellcollection.org/ at Universitetet i Oslo on November 21, 2019

Msaky, E. 2015. Oil and gas exploration - general overview. A document available at http://tpdc.co.tz/wp-content/uploads/2015/04/OIL-and-GAS-EXPLORATION.pdf.

Muhongo, S. 2013. Tanzania as an emerging energy producer. Lecture at Chatham House, The Royal Institute of International Affairs, London, 2013. A document available at https://www.chathamhouse.org/events/view/189235

Nicholas, C.J., Pearson, P.N., McMillan, I.K., Ditchfield, P.W. & Singano, J.M. 2007. Structural evolution of southern coastal Tanzania since the Jurassic. *Journal of African Earth Sciences*, **48**, 273-297.

Ohm, S.E., Karlsen, D.A. & Austin, T. 2008. Geochemically driven exploration models in uplifted areas: Examples from the Norwegian Barents Sea. *AAPG bulletin*, **92**, 1191-1223.

Palermo, D., Galbiati, M., Famiglietti, M., Marchesini, M., Mezzapesa, D. & Fonnesu, F. 2014. Insights into a new super-giant gas field-sedimentology and reservoir modeling of the Coral Reservoir Complex, Offshore Northern Mozambique. Presented at the Offshore Technology Conference-Asia, 25–28 March 2014, Kuala Lumpur, Malaysia, https://doi.org/10.4043/24907-MS.

Pereira-Rego, M.C., Carr, A.D. & Cameron, N.R. 2013. Gas success along the margin of East Africa, but where is all the generated oil? *AAPG Search and Discovery Article #10488 (2013), 1-35*, *East Africa Petroleum Province of the 21st Century Conference,* 24–26 October 2012, London. Available at http://www.searchanddiscovery.com/pdfz/documents/2013/10488pereira/ndx_pereira.pdf.html.

Peters, K. 1986. Guidelines for evaluating petroleum source rock using programmed pyrolysis. *AAPG bulletin*, **70**, 318-329.

Peters, K., Moldowan, J. & Sundararaman, P. 1990. Effects of hydrous pyrolysis on biomarker thermal maturity parameters: Monterey phosphatic and siliceous members. *Organic Geochemistry*, **15**, 249-265.

Peters, K.E. & Moldowan, J.M. 1993. *The biomarker guide: interpreting molecular fossils in petroleum and ancient sediments. Prentice Hall, Englewood Cliffs, New Jersey*.

Peters, K.E. & Cassa, M.R. 1994. Applied source rock geochemistry. *In*: Magoon, L.B. & Dow, W.G. (eds) *The Petroleum System – From Source to Trap. American Association of Petroleum Geologists Memoir, **60***, Tulsa, OK, 93-117.

Peters, K.E., Walters, C.C. & Moldowan, J.M. 2005. *The biomarker guide: biomarkers and isotopes in the environment and human history*. Cambridge University Press.

Philp, R.T. & Gilbert, T. 1986. Biomarker distributions in Australian oils predominantly derived from terrigenous source material. *Organic Geochemistry*, **10**, 73-84.

ACCEPTED MANUSCRIPT

Downloaded from http://pg.lyellcollection.org/ at Universitetet i Oslo on November 21, 2019

Purcell, P. 2014. Oil and gas exploration in East Africa: A brief history. *AAPG Search and Discovery Article #30388 (2014)*, 1-21.

Quinton, J. & Copestake, P. 2006. Mesozoic rift basins in Tanzania: Stratigraphic and structural development and petroleum potential. Poster and abstract presented at the *5th PESGB/HGS African Conference – Africa*: *The Elephants of the Future*, 12–13 September 2006, London.

Radke, M. 1987. Organic geochemistry of aromatic hydrocarbons. *In*: J. Brooks & Welte, D. (eds) *Advances in petroleum geochemistry*. Academic Press, London, **2**, 141-207.

Radke, M. 1988. Application of aromatic compounds as maturity indicators in source rocks and crude oils. *Marine and Petroleum Geology*, **5**, 224-236, http://doi.org/10.1016/0264-8172(88)90003-7.

Radke, M. & Welte, D.H. 1983. The methylphenanthrene index (MPI); a maturity parameter based on aromatic hydrocarbons. *Proceedings of the International Meeting on Organic Geochemistry*, **10**, 504-512.

Radke, M., Welte, D.H. & Willsch, H. 1982. Geochemical study on a well in the Western Canada Basin: relation of the aromatic distribution pattern to maturity of organic matter. *Geochimica et Cosmochimica Acta*, **46**, 1-10, http://doi.org/10.1016/0016-7037(82)90285-X.

Radke, M., Welte, D. & Willsch, H. 1986. Maturity parameters based on aromatic hydrocarbons: Influence of the organic matter type. *Organic Geochemistry*, **10**, 51-63.

Radke, M., Vriend, S. & Schaefer, R. 2001. Geochemical characterization of lower Toarcian source rocks from NW Germany: Interpretation of aromatic and saturated hydrocarbons in relation to depositional environment and maturation effects. *Journal of Petroleum Geology*, **24**, 287-307, http://doi.org/10.1111/j.1747-5457.2001.tb00676.x.

Rampen, S.W., Schouten, S., Abbas, B., Elda Panoto, F., Muyzer, G., Campbell, C.N., Fehling, J. & Sinninghe Damsté, J.S. 2007. On the origin of 24-norcholestanes and their use as age-diagnostic biomarkers. *Geology*, **35**, 419-422.

Reeves, C.V. 2018. The development of the East African margin during Jurassic and Lower Cretaceous times: a perspective from global tectonics. *Petroleum Geoscience*, **24**, 41-56.

Rullkotter, J., Mukhopadhyay, P.K. & Welte, D.H. 1984. GEOCHEMISTRY AND PETROGRAPHY OF ORGANIC-MATTER IN SEDIMENTS FROM HOLE 530A, ANGOLA BASIN, AND HOLE 532, WALVIS RIDGE, DEEP-SEA DRILLING PROJECT. *Initial Reports of the Deep Sea Drilling Project*, **75**, 1069-1087.

Sales, J.K. 1997. Seal strength vs. trap closure; a fundamental control on the distribution of oil and gas. *AAPG Memoir*, **67**, 57-83.

ACCEPTED MANUSCRIPT

Downloaded from http://pg.lyellcollection.org/ at Universitetet i Oslo on November 21, 2019

Sansom, P. 2018. Hybrid turbidite–contourite systems of the Tanzanian margin. *Petroleum Geoscience*, **24**, 258-276.

Schoell, M., 1983. Genetic characterisation of natural gases. *AAPG Bulletin*, 67, 2225-2238.

Seifert, W.K. & Moldowan, J.M. 1978. Applications of steranes, terpanes and monoaromatics to the maturation, migration and source of crude oils. *Geochimica et Cosmochimica Acta*, **42**, 77-95, http://doi.org/10.1016/0016-7037(78)90219-3.

Shanmugam, G. 1985. Significance of coniferous rain forests and related organic matter in generating commercial quantities of oil, Gippsland Basin, Australia. *AAPG bulletin*, **69**, 1241-1254.

Siversen, C., Schomacker, E. & Coffey, T. 2017. Cretaceous to Paleogene Deep Water Depositional Systems, Block 2, Offshore Tanzania. Abstract presented at the *Third EAGE Eastern Africa Petroleum Geoscience Forum*.

Smelror, M., Fossum, K., Dypvik, H., Hudson, W. & Mweneinda, A. 2018. Late Jurassic–Early Cretaceous palynostratigraphy of the onshore Mandawa Basin, southeastern Tanzania. *Review of Palaeobotany and Palynology*, **258**, 248-255.

Stockley, G. 1943. The Geology of the Rufiji District, Including a Small Portion of Northern Kilwa District (Matumbi Hills). *Tanganyika Notes and Records*, **16**, 7-28.

Sullivan, M.A. & Lawson, M. 2017. East Africa Gas: Source Type and maturity. Conference abstract, . *Third EAGE Eastern Africa Petroleum Geoscience Forum*.

Sutton, S., Figueredo, P., Sullivan, M., Johnson, C. & Karner, G. 2017. Tectonic History and Structural Evolution of the East Africa Margin. *Third EAGE Eastern Africa Petroleum Geoscience Forum*.

Tissot, B.P. & Welte, D.H. 1984. *Petroleum formation and occurrence, 2nd edition*. Springer-Verlag, Berlin.

Tvedt, T. (2018). Nilen (The Nile) - Historiens elv [In Norwegian]. Aschehoug, Oslo, 459p.

van Den Brink, M. 2015. *Depositional environments and mineralogical characterization of the Upper Jurassic Mitole Formation, southern Coastal Tanzania.* M. Sc. thesis, University of Oslo, 87 pp.

van Graas, G.W. 1990. Biomarker maturity parameters for high maturities: calibration of the working range up to the oil/condensate threshold. *Organic Geochemistry*, **16**, 1025-1032.

ACCEPTED MANUSCRIPT

Downloaded from http://pg.lyellcollection.org/ at Universitetet i Oslo on November 21, 2019

van Koeverden, J.H., Nakrem, H.A. & Karlsen, D.A. 2010. Migrated oil on Novaya Zemlya, Russian Arctic: Evidence for a novel petroleum system in the eastern Barents Sea and the Kara Sea. AAPG Bulletin, v. **94**, 791-817.

Volkman, J. 1988. Biological marker compounds as indicators of the depositional environments of petroleum source rocks. *Geological Society, London, Special Publications*, **40**, 103-122.

Volkman, J.K., Alexander, R., Kagi, R.I., Noble, R.A. & Woodhouse, C.W. 1983. A geochemical reconstruction of oil generation in the Barrow Sub-basin of Western Australia. *Geochimica et Cosmochimica Acta*, **47**, 2091-2105.

Weiss, H.M., Wilhelms, A., Mills, N., Scotchmer, J., Hall, P.B., Lind, K. & Brekke, T. 2000. NIGOGA-The Norwegian Industry Guide to Organic Geochemical Analyses (online). Edition 4.0, published by Norsk Hydro, Statoil, Geolab Nor, SINTEF Petroleum Research and the Norwegian Petroleum Directorate, 102 pp. Accessed on 10 October, 2018. Available at http://www.npd.no/Global/Norsk/7-Rapportering/Bronner/nigoga4.pdf.

Whaley, J. 2016. Tanzania: Largest Onshore Discovery. *GeoExPro*, Vol. **13(3)**, p.645

Whiticar, M. J., 1994. Correlation of Natural Gases with Their Sources. IN: Magoon, L. B. & Dow, W. G. (Eds.): The Petroleum system - from source to trap. *AAPG Memoir*, 60, 261-283

Wilhelms, A. & Larter, S.R. 1994. Origin of tar mats in petroleum reservoirs. Part I: introduction and case studies. *Marine and Petroleum Geology*, **11**, 418-441.

Wilkin, D. 2017. Exploration in a Low Price Environment. Conference abstract, *Third EAGE Eastern Africa Petroleum Geoscience Forum*.

Zhonghong, C., Zhi, C., Bin, C., ZiCheng, C. & Hua, L. 2019. Geochemsitry of high mature crude oil and gas from deep reservoris and its geological significance: a case study of the Shuntuoguole Lower Ulift, tarim Basin, western China, AAPG. In press.

ACCEPTED MANUSCRIPT

Downloaded from http://pg.lyellcollection.org/ at Universitetet i Oslo on November 21, 2019

APPENDIX 1

Stratigraphy and sedimentology

Section WP92

Section WP92 is located in the North Mandawa area (Figs 1, 2 and 3) where approximately 25 meters of the Kipatimu Formation (Fig. 4) is exposed in a narrow drainage gully along a dirt road. Section WP92 (Fig. 4) can be divided into three parts based on facies associations: Lower part (0–6.3 m), middle part (6.3–9.8m) and upper part (9.8–24.7 m). The palynomorph assemblages of claystones from the lower part of the section yielded Late Jurassic depositional ages, whereas the upper part of the section shows a possible Early Cretaceous age, not older than Albian (Smelror *et al*. 2018). The Cretaceous part of the Kipatimu Formation has not previously been described in the Mandawa Basin.

The lower part of the section commences with white-pinkish friable sandy siltstone overlain by purple and greenish-gray claystone in turn overlain by sandstones. These sandstones are medium to coarse grained, planar laminated or cross-bedded with rip-up clay clasts. The colors are red to yellowish-red. The sandstones are overlain by light greenish-gray claystones.

The middle part of the section consists of conglomerates and sandstones. The basal conglomerate, one meter thick, is polymictic and grain supported with a coarse to medium grained matrix. The contact towards the clay bed below is wavy. The conglomerate is composed of large (up to 53 cm) sandstone clasts, siliciclastic and carbonate claystones, well-rounded quartz and chert clasts and some basement fragments. Some glauconite grains were observed in the matrix (Table 1). The conglomerate is succeeded by upwards fining friable pinkish sandstones (sample WP92-11-14), deposited after the conglomerate was lithified by calcite cementation. On top of this sandstone sits a second conglomerate bed (30 cm thick) with similar characteristics as the conglomerate below. The main difference is that the clast size is smaller in this upper conglomerate, which has sharp, irregular contacts to underlying and overlying sandstone beds. The overlying sandstone appears comparable to sandstones from within the conglomerate, and shows sign of bioturbation. The sandstone is succeeded by 50 cm of bioturbated greenish-gray

ACCEPTED MANUSCRIPT

Downloaded from http://pg.lyellcollection.org/ at Universitetet i Oslo on November 21, 2019

claystone and capped by 75 cm of fine grained yellowish sandstone with discontinuous clay lenses (Fig. 4).

The upper part of the section (Fig. 4) is dominated by claystones intercalated with thin very fine grained sandstone beds. The section is poorly exposed and partly covered by loose sediments. Two thick sandstone beds separated by mudstone were found at 12.25 to 13.25 meter. The lower bed (level 12.25–12.50 m) has discontinuous parallel laminations, whereas the upper bed (13.25–13.25 m) is homogenous at the base, parallel laminated in the middle part (sample WP92-13-14) and displays climbing ripples in the upper part.

A thin fine grained, rippled sandstone bed (level 23.20 m) sits on top of the alternating sequence of clay and very fine sandstone beds. The sandstone (sample WP92-19-14) contains articulated bivalves and is bioturbated, indicating deposition in marine influenced environment. Thin section studies revealed abundant shell and echinoderm fragments plus fecal pellets and some rare ooids (Table 1). This sandstone is in turn overlain by 135 cm of seemingly structureless and weathered dark gray claystone. On top of the section sits a new conglomerate bed, approximately 60 cm thick. This conglomerate is calcite cemented and, as opposed to the conglomerate beds located below (in between level 6 and 9) and described above, it contains abundant articulated and disarticulated bivalves and gastropods. Bioturbation is common, and Diplocraterion trace fossils were also observed. The conglomerate clasts are mainly of sedimentary origin.

ACCEPTED MANUSCRIPT

Section NQ

At locality NQ (Figs 3 and 4) both members of the Lower Cretaceous Nalwehe Formation, are exposed and display a regressive development; from shallow marine carbonaceous conditions to siliciclastic dominated, marine sedimentation (Figs 3 and 4). The NQ section comprises two sections: NQ1 and NQ2.

The Nalwehe Limestone Member in the NQ1 section commences with a well cemented 1m thick mudstone (sample NQ1-1-14; Fig. 4; Table 1) which grades into a

Downloaded from http://pg.lyellcollection.org/ at Universitetet i Oslo on November 21, 2019

wackestone (NQ1-3-14) as the bioclastic content increases upwards. At the 2 meter level colonial and solitary corals and articulated gastropods were identified and the rock is grain-supported and can be classified as a packstone. From this level and upwards there is an increase in both diversity and amount of bioclastic material, and the packstone grades into a grainstone. From the 4.5 meter level and to the top limestone surface, at 6.30 meter, corals are found in situ, and fossils are mainly articulated. The mudstones and wackestones of Nalwehe Limestone Member are mainly composed of micrite and scattered fossils and are interpreted to be deposited in a low energy lagoonal environment (Haid, 2018). The presence of framboidal pyrite in sample NQ1-1-14 suggests a semi-restricted environment with partly reducing conditions. There is an upward increase in the amount of sparitic calcite cement, suggesting more ventilated depositional conditions. The topmost Nalwehe Member packstones contain in situ corals and large marine diversity, indicating patch reef conditions in the distal parts of the shallow subtidal lagoon (sample NQ1-1-14). The uppermost part of the Nalwehe Limestone Member displays a highly irregular karstification surface (Baremian unconformity?). Cavities and holes were later filled and capped by very coarse fossil-rich sand. The overlying sandstones (3.5 meter thick) belong to the Nalwehe Sandstone Member.

The Nalwehe Sandstone Member section starts with a 1.8 meter of very fine grained friable sandstone (NQ1-7-14; Fig.4; Table 1) with scattered coal fragments. At level 8.20 meter to the top the soft and friable sandstone are cross-bedded and alternates with thin (4-6 cm) fine-grained, carbonate-cemented beds (Fig. 4). Haid (2018) interpret the Nalwehe Sandstone Member to represent clastic, shallow marine environments, a basinal facies shift relative to the underlying carbonates.

The NQ2 section comprises only the Nalwehe Limestone Member (Fig. 4) and is believed to represent more proximal facies compared to the NQ1 section. One sample from the NQ2 section has been analysed (sample NQ2-2-14, Fig. 4). Sample NQ2-2-14 is a silty claystone interbedded between a stromatolittic packstone and oncoid-bearing grainstone (Fig. 4). The stratigraphic position of NQ2 relative to the NQ1 section was not resolved due to the complex faulting within the quarry complex.

ACCEPTED MANUSCRIPT

Downloaded from http://pg.lyellcollection.org/ at Universitetet i Oslo on November 21, 2019

Section MKW

A cliff section of the Nalwehe Sandstone Member has been carved out by one of the tributaries of the Mbwemkuru River, the present locality MKW (Figs 2, 4 and 6). The logged section is 10.4 meters thick and consists of trough cross-bedded, gray, fine to coarse-grained carbonate cemented sandstones (Figs 3, 4 and 6).

Trough cross-bedded units (20 to 100 cm thick) have conglomeratic lower parts towards erosive bases, and are further interbedded in parts by parallel laminated and massive beds. Most of the cross-beds have unidirectional dips showing transport towards the southwest, but some beds display bidirectional cross-bedding.

The sediment composition is immature with high feldspar, amphibole and rock fragment contents, which can be classified as lithic arkose. The dominant grain shapes are angular to sub-angular, reflecting fairly short sediment transportation. The presence of shell fragments further suggests that the sediments were deposited during marine conditions.

ACCEPTED MANUSCRIPT

Downloaded from http://pg.lyellcollection.org/ at Universitetet i Oslo on November 21, 2019

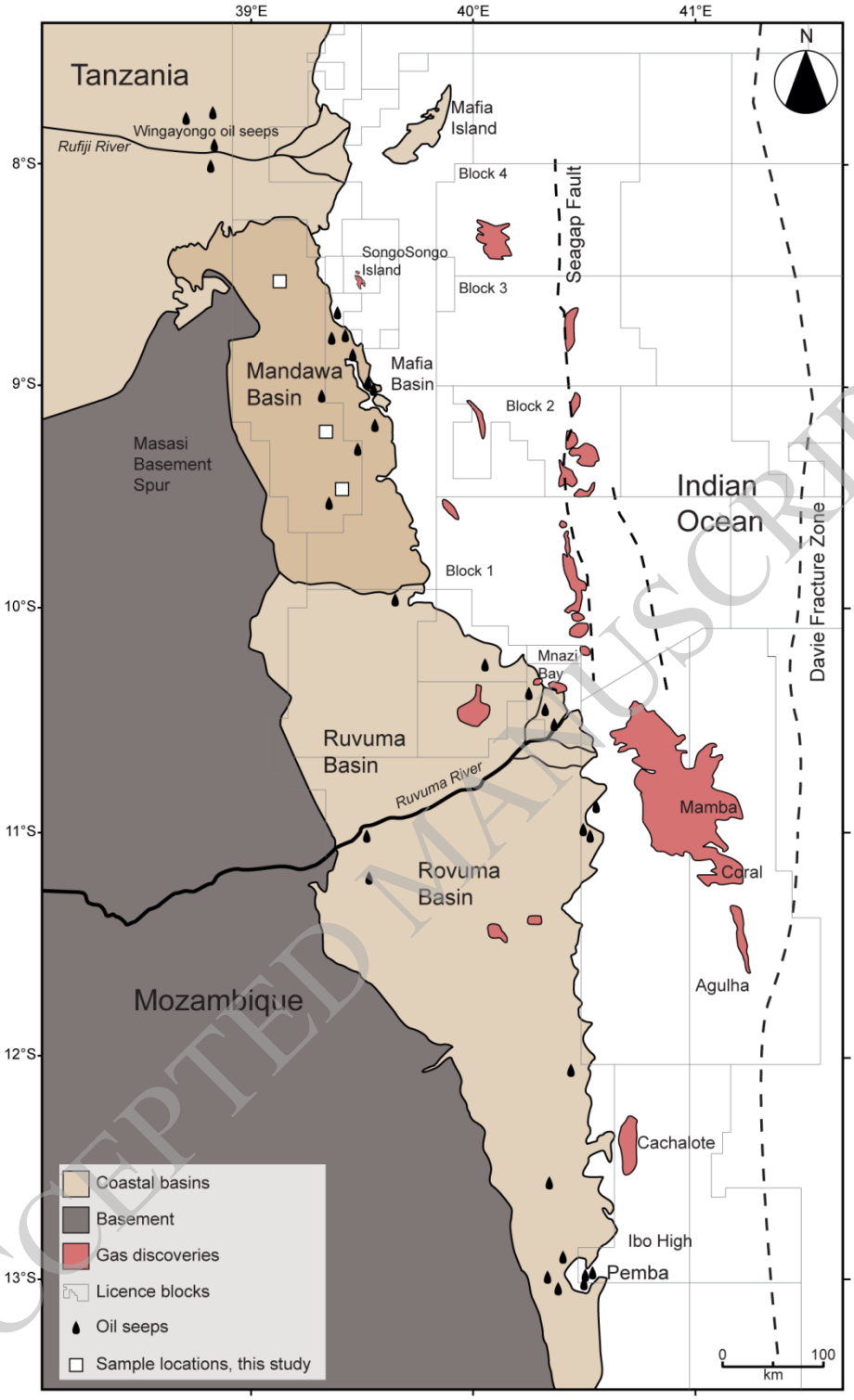

ACCEPTED MANUSCRIPT

Downloaded from http://pg.lyellcollection.org/ at Universitetet i Oslo on November 21, 2019

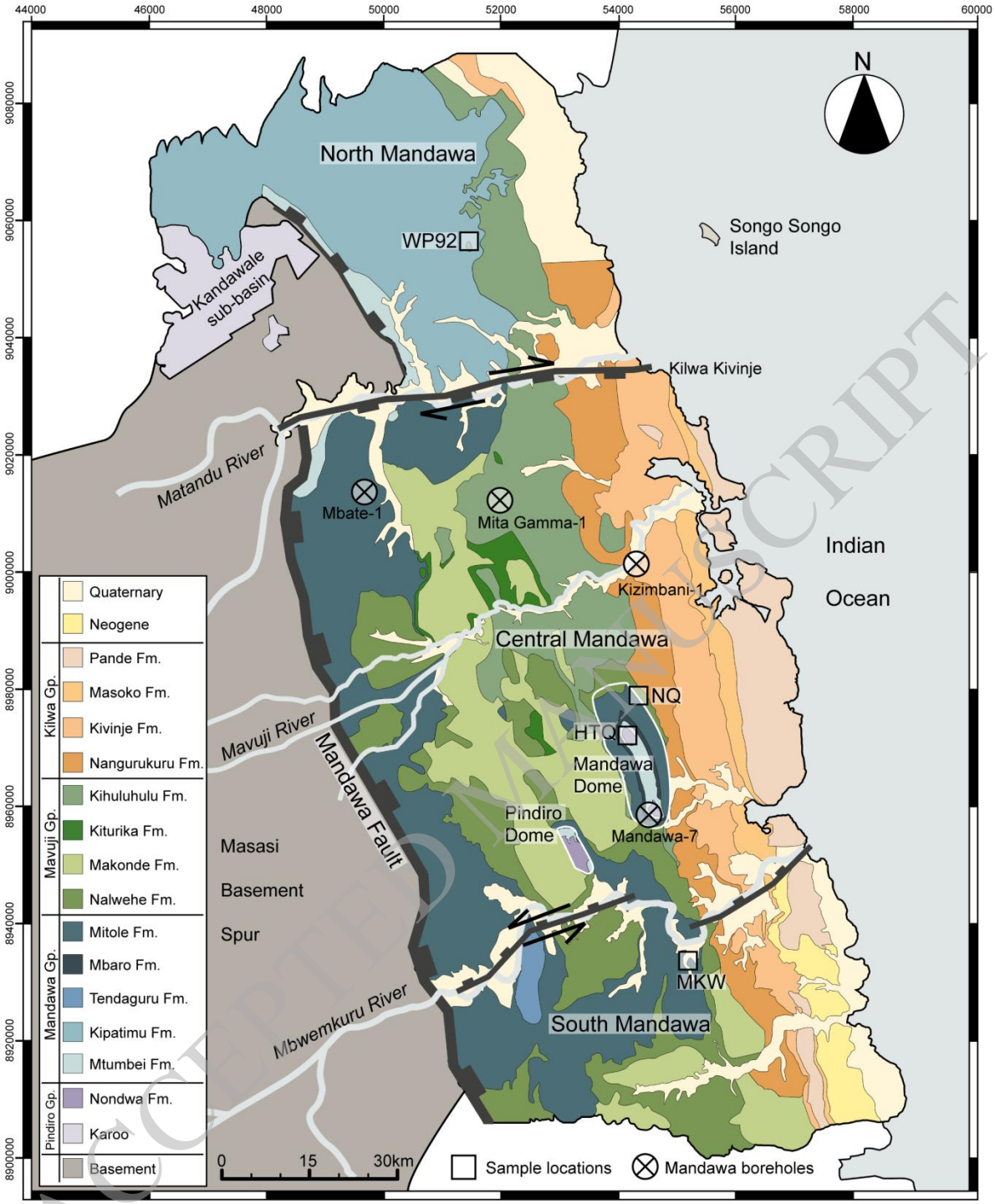

ACCEPTED MANUSCRIPT

Downloaded from http://pg.lyellcollection.org/ at Universitetet i Oslo on November 21, 2019

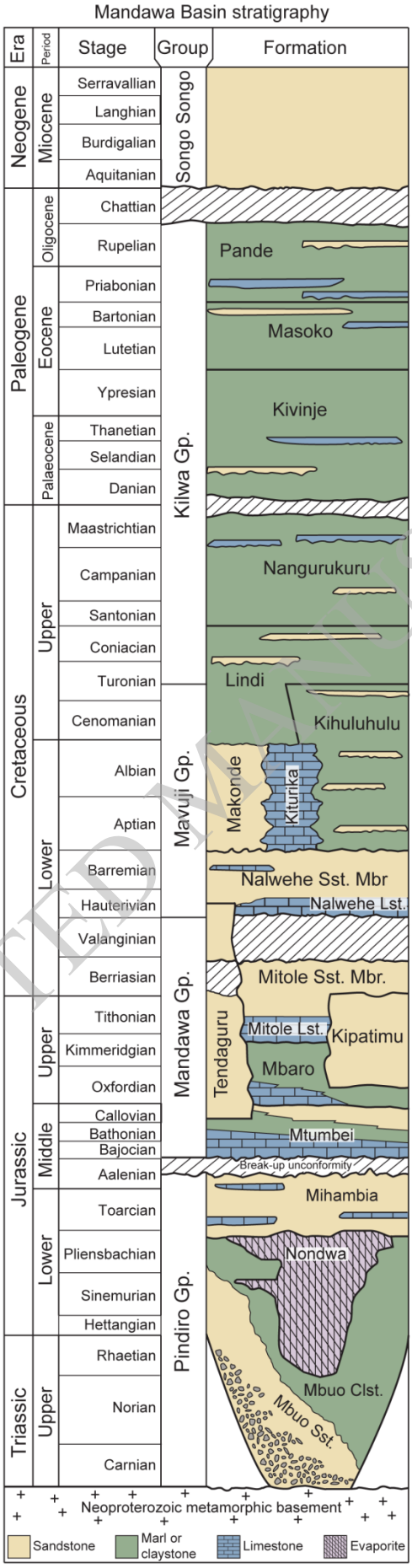

ACCEPTED MANUSCRIPT

Downloaded from http://pg.lyellcollection.org/ at Universitetet i Oslo on November 21, 2019

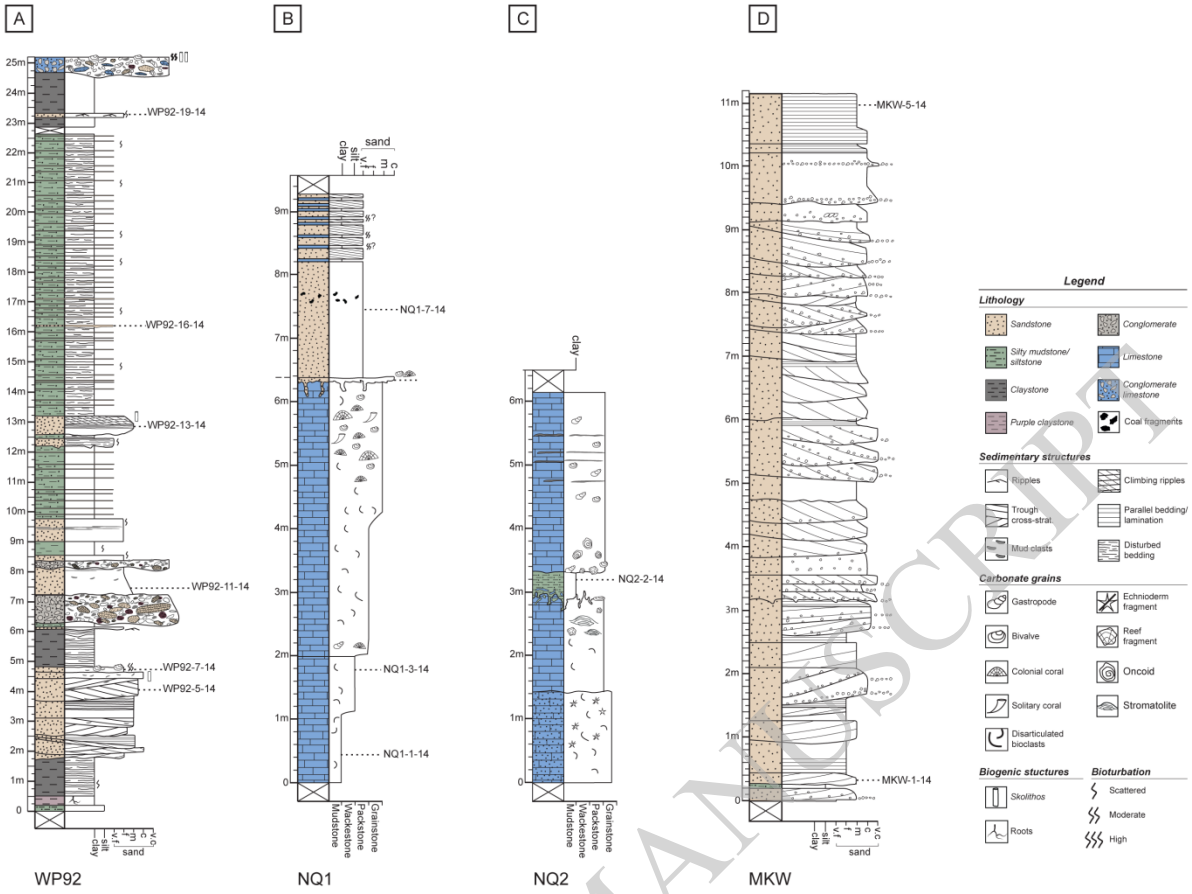

ACCEPTED MANUSCRIPT

Downloaded from http://pg.lyellcollection.org/ at Universitetet i Oslo on November 21, 2019

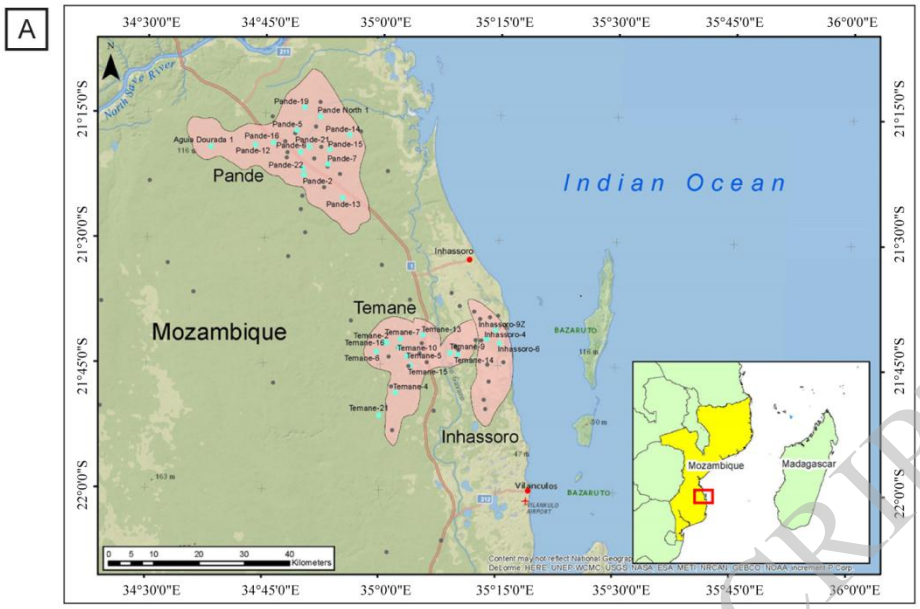

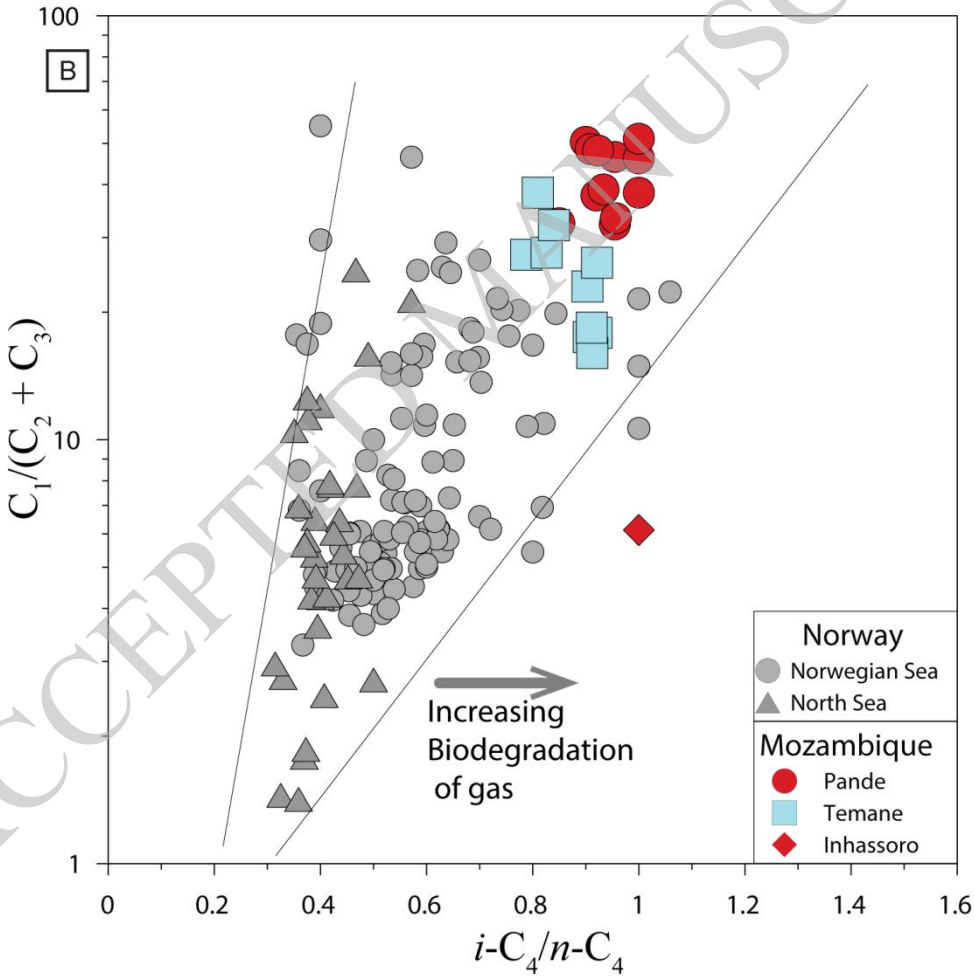

ACCEPTED MANUSCRIPT

Downloaded from http://pg.lyellcollection.org/ at Universitetet i Oslo on November 21, 2019

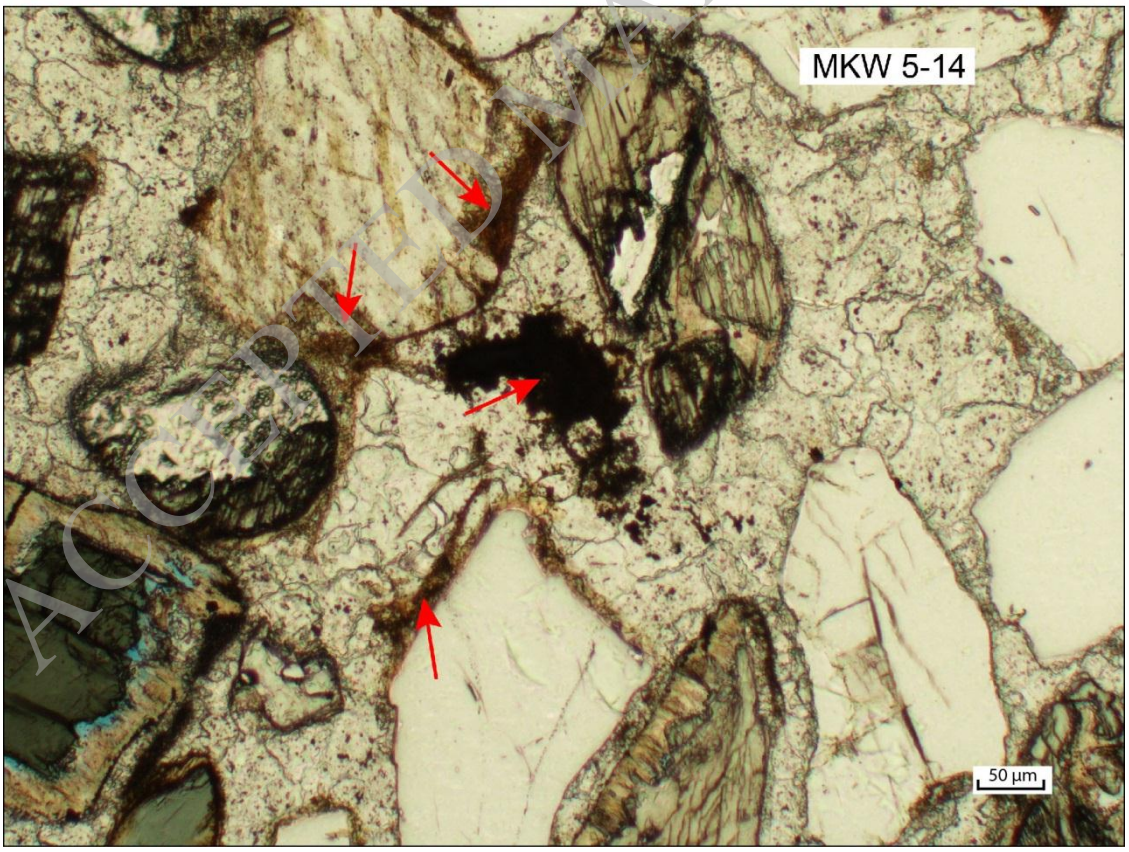

ACCEPTED MANUSCRIPT

Downloaded from http://pg.lyellcollection.org/ at Universitetet i Oslo on November 21, 2019

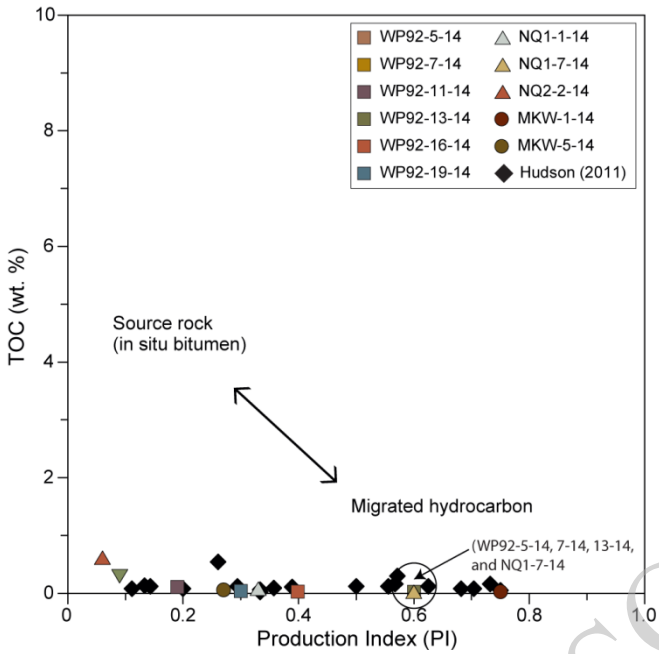

ACCEPTED MANUSCRIPT

Downloaded from http://pg.lyellcollection.org/ at Universitetet i Oslo on November 21, 2019

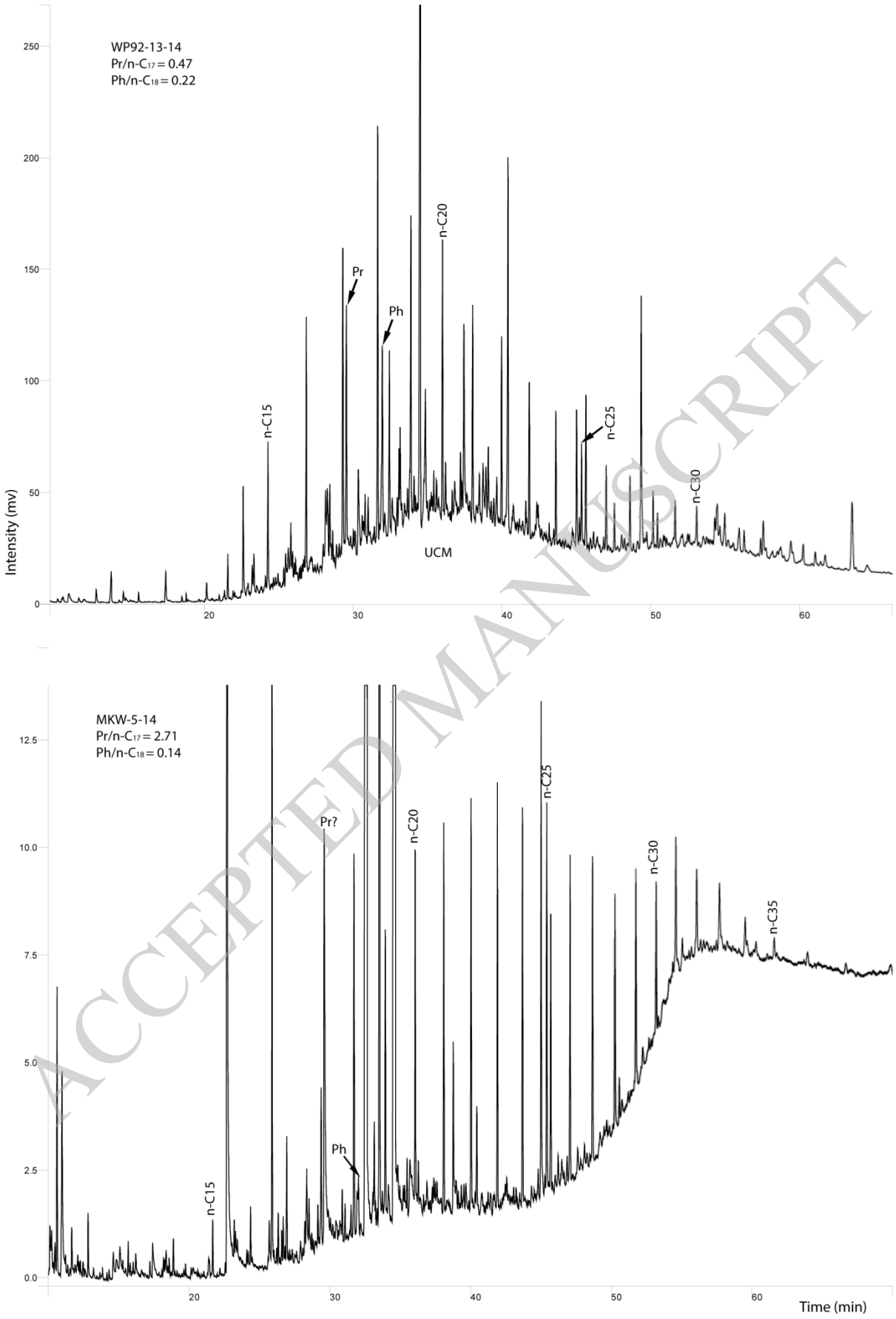

ACCEPTED MANUSCRIPT

Downloaded from http://pg.lyellcollection.org/ at Universitetet i Oslo on November 21, 2019

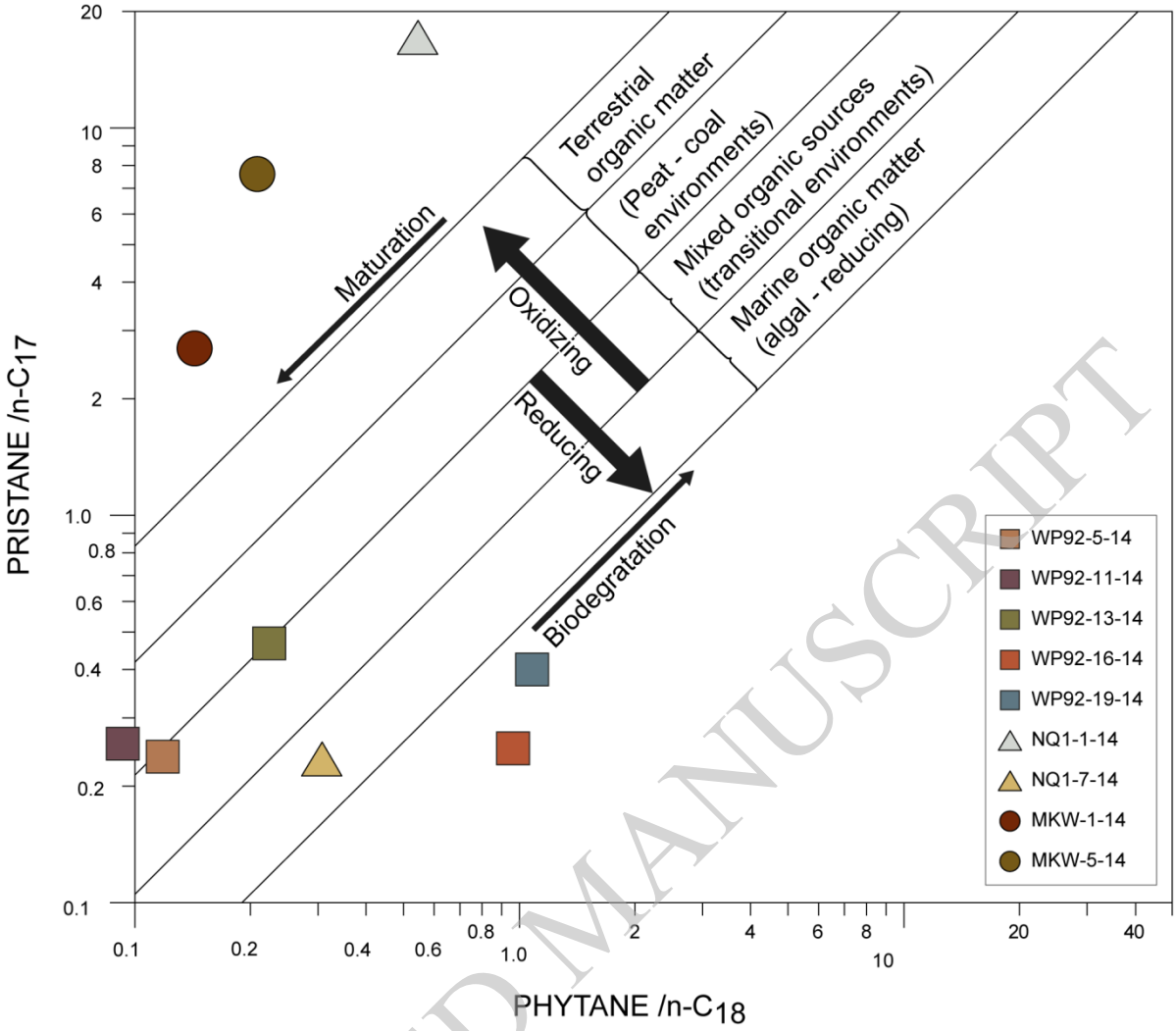

ACCEPTED MANUSCRIPT

Downloaded from http://pg.lyellcollection.org/ at Universitetet i Oslo on November 21, 2019

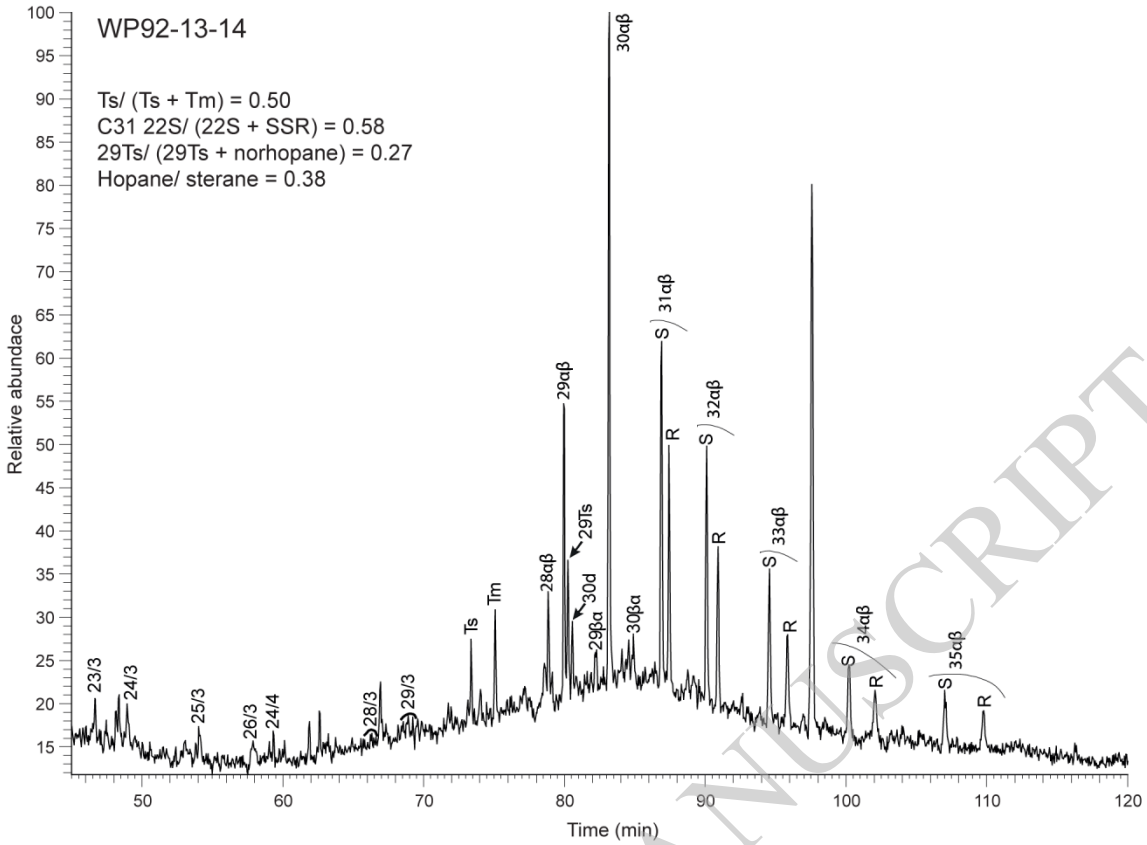

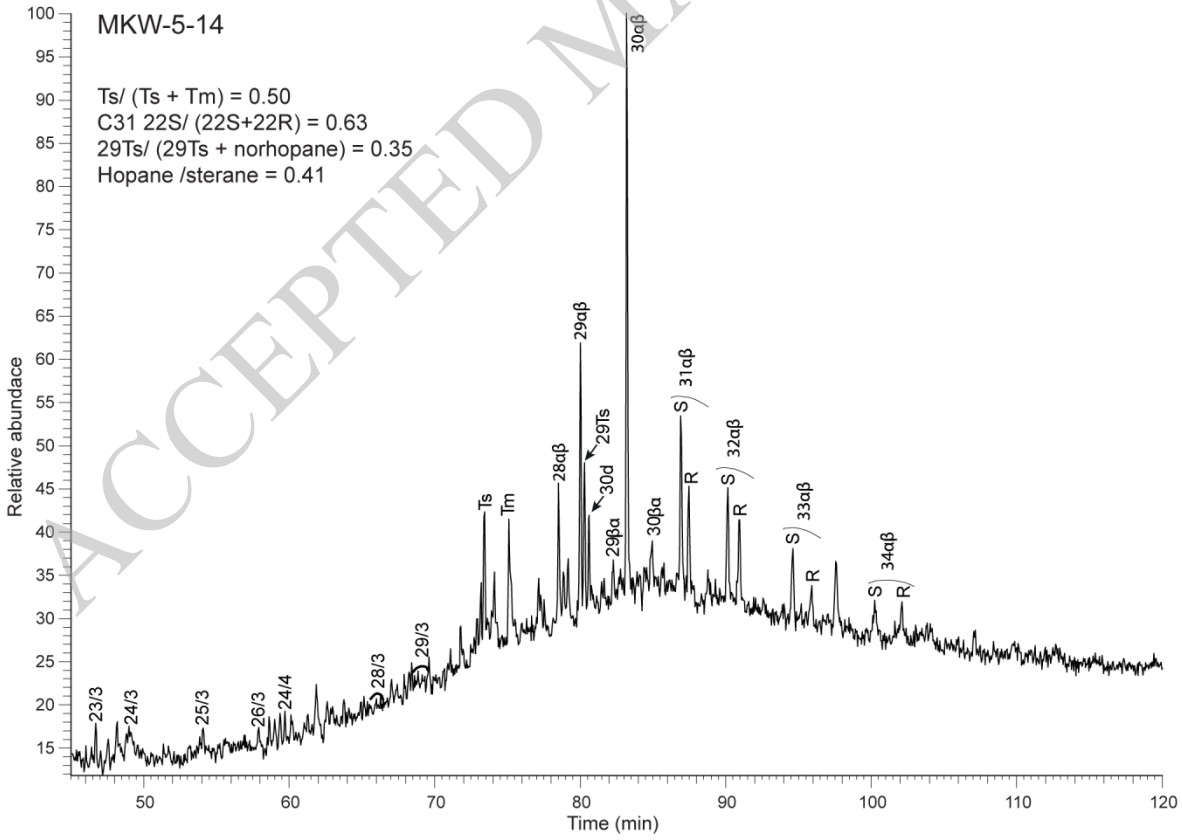

ACCEPTED MANUSCRIPT

Downloaded from http://pg.lyellcollection.org/ at Universitetet i Oslo on November 21, 2019

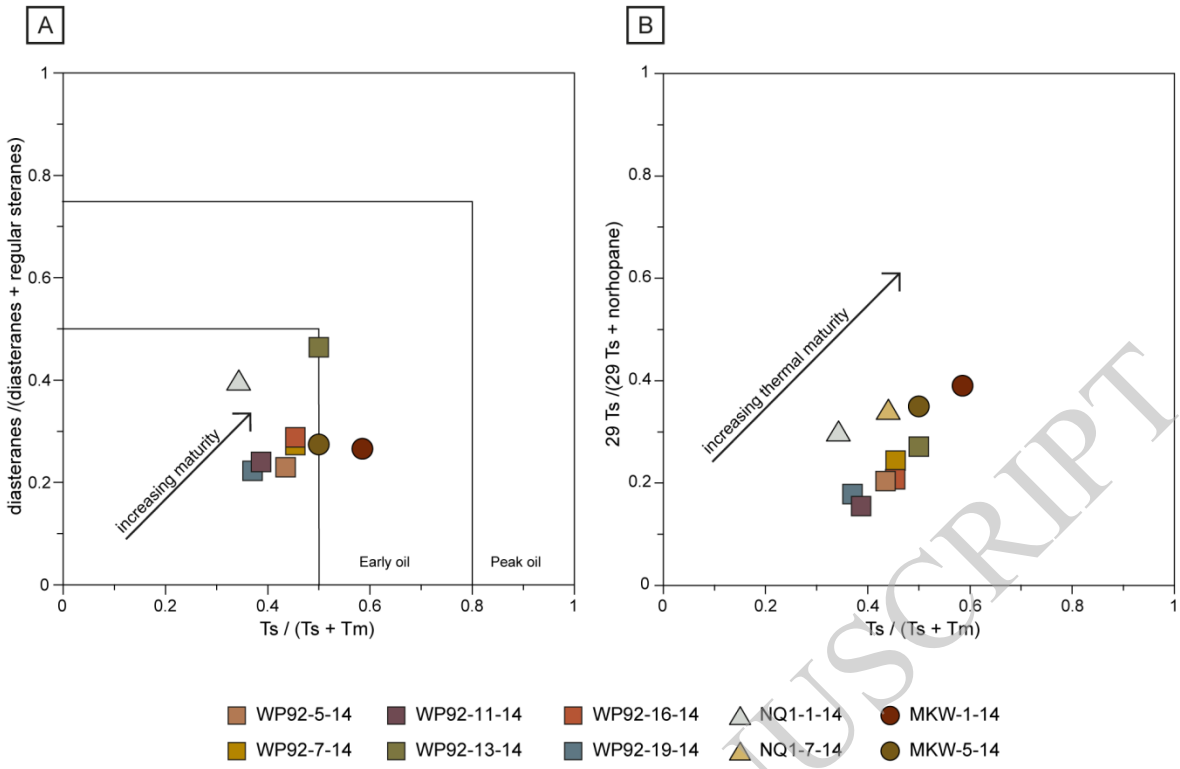

ACCEPTED MANUSCRIPT

Downloaded from http://pg.lyellcollection.org/ at Universitetet i Oslo on November 21, 2019

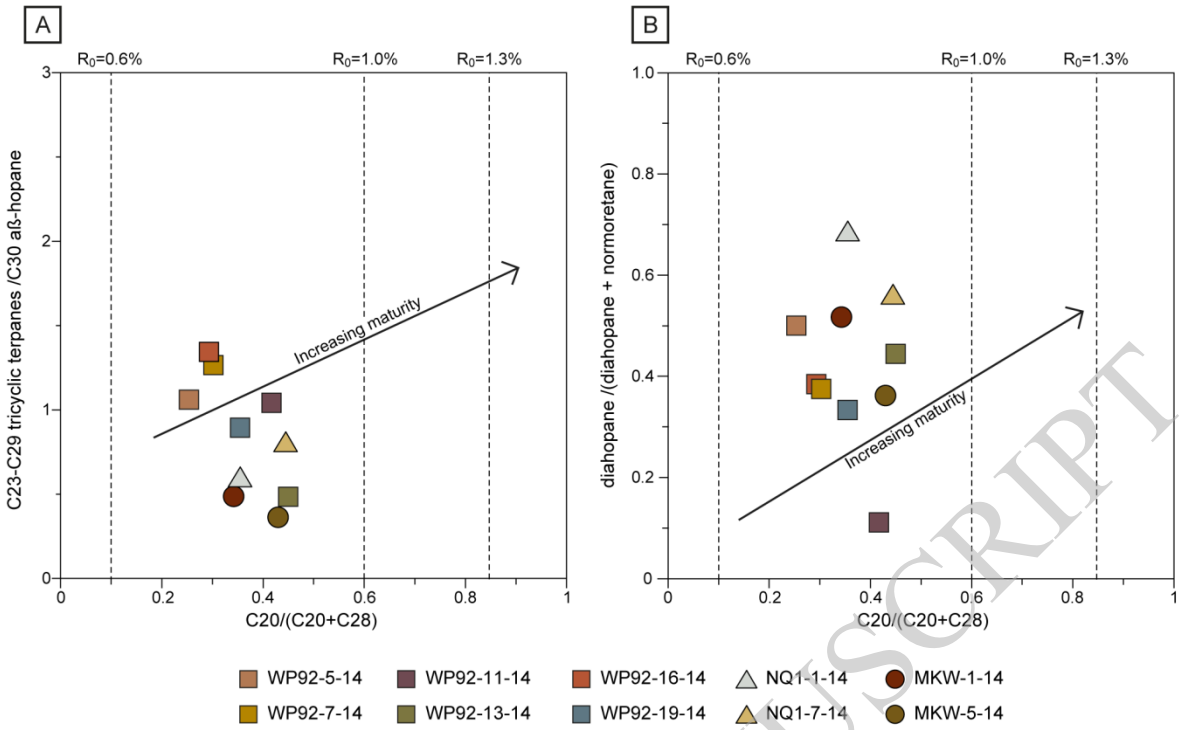

ACCEPTED MANUSCRIPT

Downloaded from http://pg.lyellcollection.org/ at Universitetet i Oslo on November 21, 2019

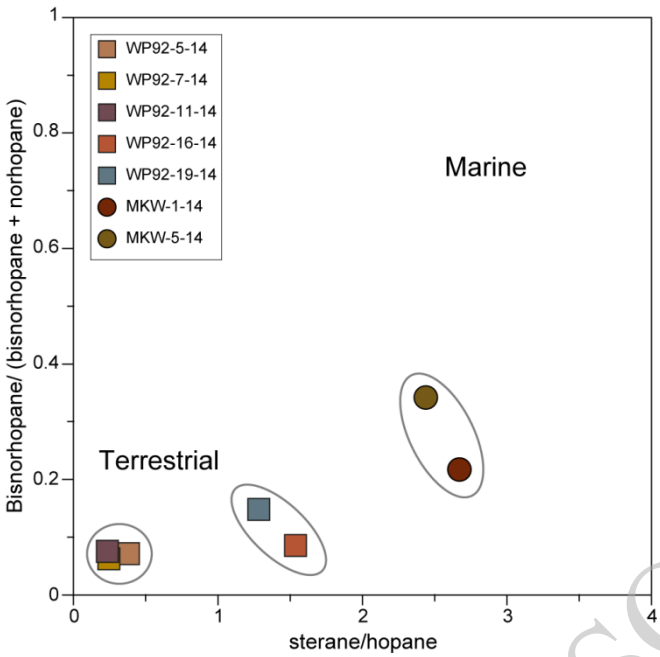

ACCEPTED MANUSCRIPT

Downloaded from http://pg.lyellcollection.org/ at Universitetet i Oslo on November 21, 2019

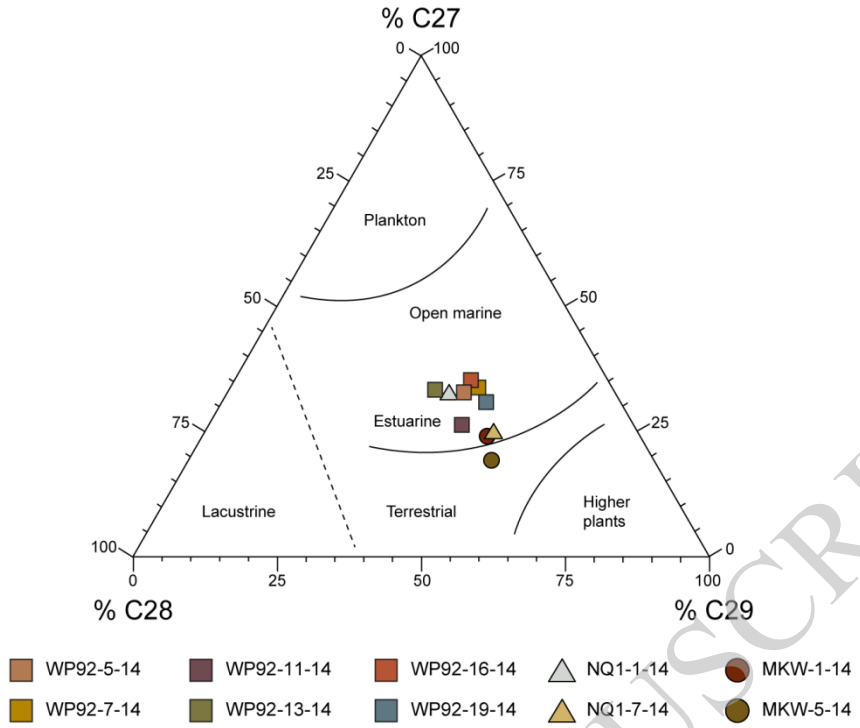

ACCEPTED MANUSCRIPT

Downloaded from http://pg.lyellcollection.org/ at Universitetet i Oslo on November 21, 2019

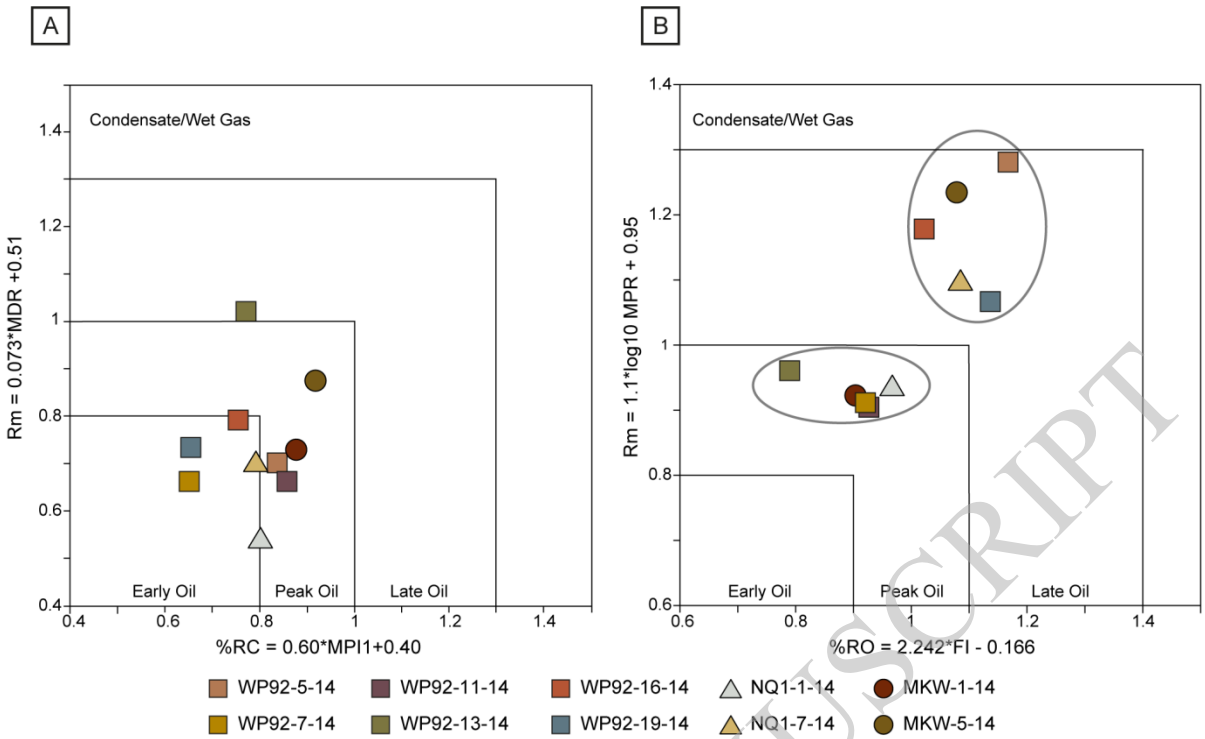

ACCEPTED MANUSCRIPT

Downloaded from http://pg.lyellcollection.org/ at Universitetet i Oslo on November 21, 2019

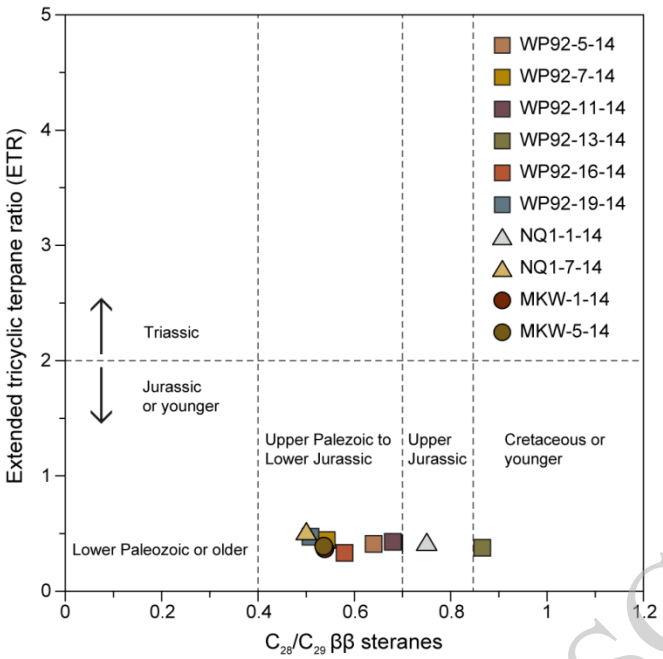

ACCEPTED MANUSCRIPT

Downloaded from http://pg.lyellcollection.org/ at Universitetet i Oslo on November 21, 2019

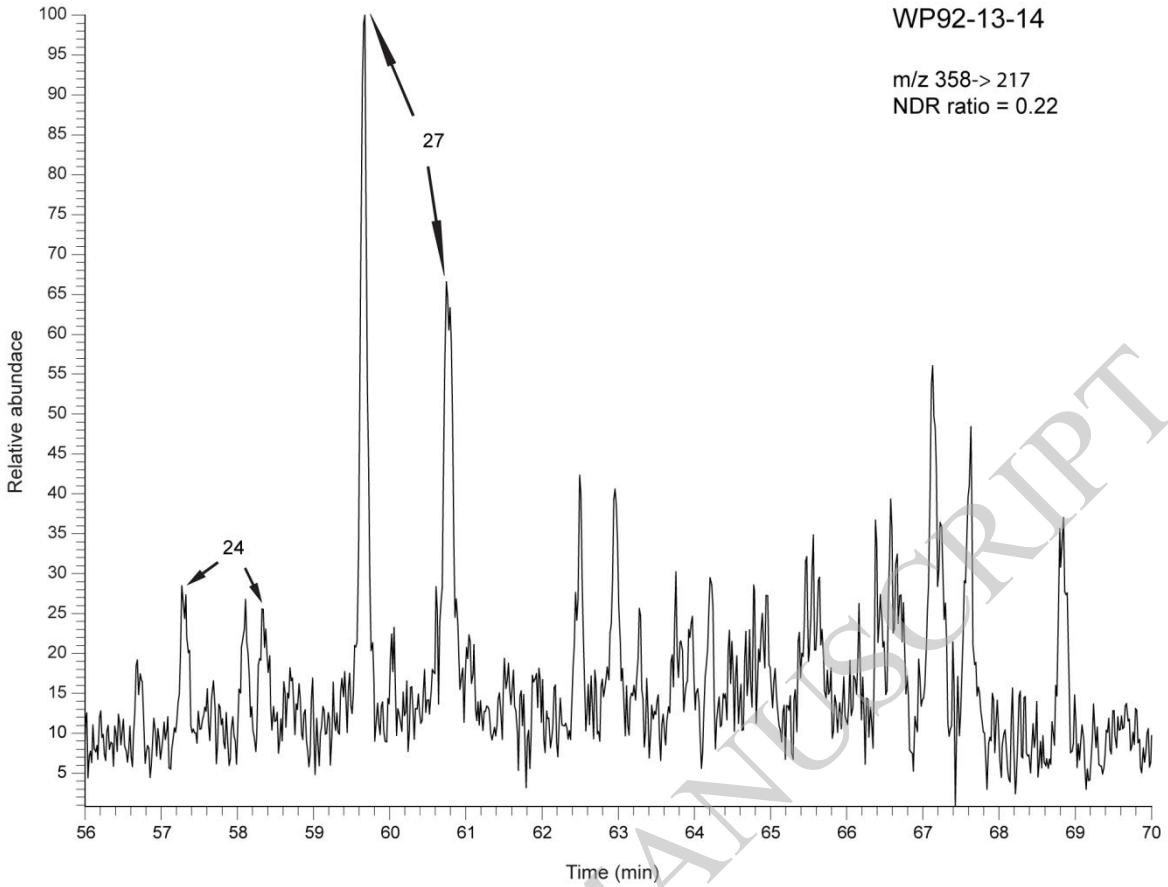

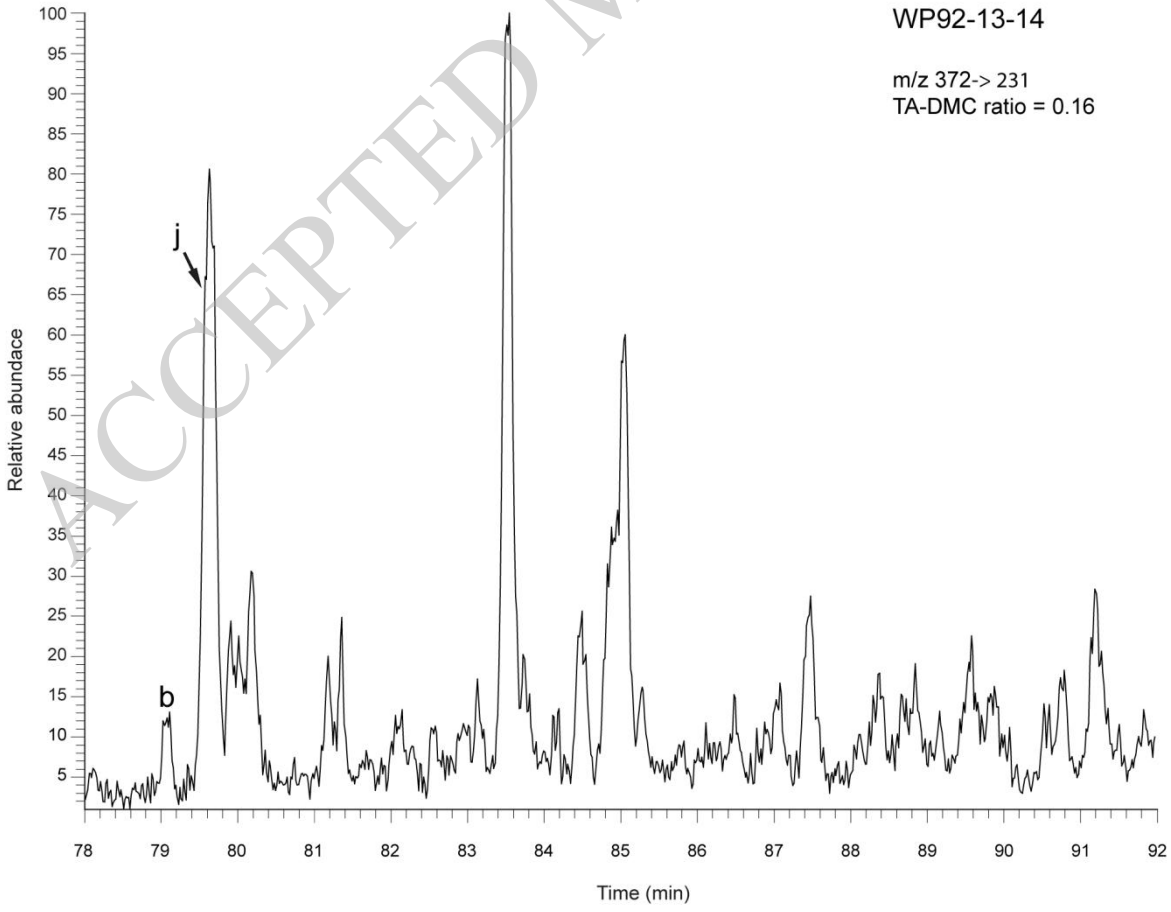

ACCEPTED MANUSCRIPT

Table 1. Sample overview

Age and Formation	Sample	Rock type	Sampled bed - grain size/sorting/colour/structures	Petrography - grain shape/contacts/fossils
Upper Jurassic Kipatimu Fm.	WP92-5-14	Subarkosic wacke	Fine-grained, moderately sorted, yellowish-brown, trough cross-bedded sandstone with clay rip-up clasts.	Sub-angular to sub-rounded grain shapes, tangential to long grain contacts. Some grain are smectite coated. Calcite cemented and minor micro-quartz cement. Later stage calcite and feldspar dissolution - secondary porosity partially filled with authigenic kaolinite.
	WP92-7-14	Litharenite	Very fine-grained, poorly sorted, brownish-gray sandstone with clay mud clasts, articulated shells and vertical burrows.	Angular to rounded grain shapes, floating to point grain-contacts. Contains abundant lithoclasts of mostly mudrocks, scattered faecal pellets and ooids, and common (mostly) disarticulated fossils. Some larger shells have been bored after deposition.
Lower Cretaceous ? Kipatimu Fm.	WP92-11-14	Subarkose	Fine-grained, moderately sorted, brownish-gray sandstone with green mudclasts.	Sub-angular to rounded, long to convex-concave grain contacts. Quartz cemented. Secondary porosity caused by late stage feldspar dissolution partially or completely filled with authigenic clay.
	WP92-13-14	Quartz arenite	Medium-grained well-sorted, yellowish-brown sandstone. Parallel bedded and climbing ripple laminated.	Grain shape difficult to determine due to quartz overgrowths. Convexo-concave and long grain contacts. Quartz and calcite cemented. Later stage calcite and feldspar dissolution - authigenic kaolinite in secondary pore spaces, and iron oxide cement. Rich in organic material (twigs, charcoal, algal remains).
	WP92-16-14	Arkose	Very fine-grained, well sorted, well cemented gray sandstone.	Rounded to sub-angular grain shapes, floating to tangential grain contacts. Sparry calcite cemented, quartz overgrowths. Rare and small, abraded fossil fragments.
	WP92-19-14	Arkose	Fine-grained moderately sorted brownish-gray sandstone. Sinuous asymmetric current ripple lamination. Minor bioturbation.	Sub-angular to sub-rounded grain shapes, tangential to long grain contacts, sparry calcite cemented, quartz overgrowths. Common rounded chert grains. Scattered fossil fragments.
Lower Cretaceous Nalwehe Fm.	NQ1-1-14	Mudstone	Crystalline light gray matrix supported limestone with scattered fossil fragments.	Fossils floating in micritic mud; some are disarticulated. Common fossil types include: echinoderm, sponge spicules, mussels. Most fossils are strongly recrystallized with sparry calcite. Minor pyrite and dolomite were detected.
	NQ1-3-14	Wackestone	Similar to NQ1-1-14.	Contains more bioclasts than NQ1-1-14.
	NQ1-7-14	Arkosic Wacke	Very fien-grained, moderately well Sorted, yellowish-brown friable sandstone. No sedimentary structures. Scattered coal fragments.	Angular to sub-rounded, tangential to long contacts. Rich in depositional mud (53%) and contains 18% smectite.
	NQ2-2-14	Silty claystone	Carbonate cemented.	No fossil was observed.
Lower Cretaceous Nalwehe Fm.	MKW-1-14	Lithic arkose	Fine-grained sandstone, moderately well sorted. Carbonate cemented. Trough cross-bedded sandstone.	Grain supported, fine- to medium-grained, angular to sub-angular, some amphibole grains are partially or fully dissolved and replaced by smectite. Rare small abraded fossil fragments (shells and echinoderm).

ACCEPTED MANUSCRIPT

MKW-5-14	Lithic arkose	Medium-grained sandstone, moderately well sorted. Carbonate cemented. Parallel laminated sandstone	Angular to sub-angular grain shapes, floating to tangential grain contacts. Amphibole grains are less dissolved than in sample MKW-1-14. Smectite in secondary pore spaces, and minor late iron oxide cement.

ACCEPTED MANUSCRIPT

Table 2. TOC and Rock-Eval data

TOC, total organic carbon; S1, free hydrocarbon (mg HC/ g rock); S2, hydrocarbon generated during pyrolysis (mg HC/ g rock); Tmax, temperature at maximum hydrocarbon generation during pyrolysis (temp. °C of S2 peak); PP, Petroleum Potential (PP = S1 + S2); HI, Hydrogen index (mg HC/ g TOC); PI, production index (PI = S1/S1 +S2).
*TOC content is too low for to perform a valid Rock-Eval pyrolysis.

Sample ID	Sample type	S1 (mg g^{-1})	S2 (mg g^{-1})	S3 (mg g^{-1})	Tmax (°C)	PP (mg g^{-1})	PI	HI (mg g^{-1})	OI (mg g^{-1})	TOC (%)*
MKW-1-14	Outcrop	0.06	0.02	0.1	-	0.08	0.75	159	-	0.01*
MKW-5-14	Outcrop	0.01	0.04	-	456	0.05	0.20	73	-	0.06
NQ1-1-14	Outcrop	0.05	0.10	0.19	442	0.15	0.33	100	190	0.10
NQ1-3-14	Outcrop	0.01	0.07	1.55	449	0.08	0.13	6	137	1.13
NQ1-7-14	Outcrop	0.03	0.02	0.13	385	0.05	0.60	160	-	0.01*
NQ2-2-14	Outcrop	0.02	0.32	1.76	366	0.34	0.06	50	274	0.64
WP92-5-14	Outcrop	0.03	0.02	0.12	-	0.05	0.60	157	-	0.01*
WP92-7-14	Outcrop	0.03	0.02	0.11	436	0.05	0.60	55	301	0.04
WP92-11-14	Outcrop	0.03	0.13	0.19	369	0.16	0.19	118	173	0.11
WP92-13-14	Outcrop	0.03	0.02	0.11	378	0.05	0.60	72	399	0.03
WP92-16-14	Outcrop	0.02	0.03	0.12	444	0.05	0.40	71	286	0.04
WP92-19-14	Outcrop	0.03	0.07	0.09	364	0.1	0.30	177	227	0.04
HTQ1-14	Outcrop	0.02	0.21	-	434	0.23	0.09	82	-	0.25

ACCEPTED MANUSCRIPT

Table 3. Maturity and facies parameters calculated from GC-FID and GC-MS chromatograms

Sample ID	Sample type	1	2	3	4	5	6	7	8	9	10	11	12	13	14	15	16	17	18
MKW-1-14	Outcrop	0.59	0.52	0.60	0.87	0.39	0.22	0.49	0.09	2.67	0.53	0.40	0.27	24.05	26.58	49.37	0.34	0.66	0.94
MKW-5-14	Outcrop	0.50	0.70	0.63	0.92	0.35	0.34	0.36	0.05	2.44	0.65	0.28	0.27	19.23	28.21	52.56	0.43	0.72	1.81
NQ1-1-14	Outcrop	0.34	0.69	0.58	0.89	0.30	0.51	0.60	0.06	-	0.38	0.39	0.40	32.77	28.81	38.42	0.35	-	0.98
NQ1-7-14	Outcrop	0.44	0.56	0.65	0.83	0.34	0.23	0.81	0.14	-	-	-	-	25.00	25.00	50.00	0.44	0.89	1.37
WP92-7-14	Outcrop	0.45	0.38	0.60	0.85	0.24	0.06	1.26	0.18	0.24	0.55	0.29	0.27	33.74	23.31	42.94	0.30	0.94	0.92
WP92-5-14	Outcrop	0.43	0.50	0.60	0.84	0.20	0.07	1.06	0.12	0.38	0.59	0.39	0.23	32.79	26.23	40.98	0.25	0.95	2.00
WP92-11-14	Outcrop	0.39	0.11	0.61	0.87	0.16	0.08	1.04	0.17	0.23	0.54	0.42	0.24	26.32	29.82	43.86	0.42	0.60	0.91
WP92-13-14	Outcrop	0.50	0.44	0.58	0.92	0.27	0.25	0.49	0.07	2.66	0.50	0.53	0.46	33.33	30.92	35.74	0.45	0.67	1.02
WP92-16-14	Outcrop	0.45	0.38	0.58	0.89	0.21	0.09	1.34	0.20	1.54	0.53	0.32	0.29	35.25	23.75	41.00	0.29	0.80	1.61
WP92-19-14	Outcrop	0.37	0.33	0.63	0.86	0.18	0.15	0.89	0.12	1.28	0.57	0.38	0.22	30.83	23.33	45.83	0.35	0.69	1.28

ACCEPTED MANUSCRIPT

Table 3 (continued). Maturity and facies parameters calculated from GC-FID and GC-MS chromatograms

Sample Id	Sample type	19	20	21	22	23	24	25	26	27	27	28	29	30	31	32	33	34
MKW-1-14	Outcrop	0.80	0.43	3.00	0.92	0.88	0.80	0.73	3.68	0.24	0.24	7.60	0.21	15.20	0.41	0.64	-	-
MKW-5-14	Outcrop	0.86	0.51	5.00	1.23	0.92	0.98	0.88	2.54	0.25	0.25	2.71	0.14	7.64	0.47	0.51	-	-
NQ1-1-14	Outcrop	0.67	0.46	0.45	0.94	0.80	0.87	0.54	1.54	1.22	1.22	16.60	0.55	13.83	0.43	0.68	-	-
NQ1-7-14	Outcrop	0.65	0.51	2.67	1.10	0.79	0.98	0.70	3.23	0.35	0.35	0.24	0.31	0.75	0.59	0.49	-	-
WP92-7-14	Outcrop	0.42	0.44	2.10	0.91	0.65	0.82	0.66	0.95	0.87	0.87	-	-	-	0.59	0.49	-	-
WP92-5-14	Outcrop	0.73	0.55	2.63	1.28	0.84	1.07	0.70	1.76	0.44	0.44	-	-	-	0.37	0.54	-	-
WP92-11-14	Outcrop	0.76	0.44	2.10	0.90	0.86	0.83	0.66	3.62	0.26	0.26	0.26	0.09	1.50	0.37	0.54	-	-
WP92-13-14	Outcrop	0.62	0.38	7.00	0.96	0.77	0.69	1.02	0.60	0.46	0.46	0.47	0.22	0.82	0.52	0.50	0.22	0.16
WP92-16-14	Outcrop	0.59	0.49	3.86	1.18	0.75	0.92	0.79	0.48	0.89	0.89	0.25	0.96	0.09	0.38	0.87	-	-
WP92-19-14	Outcrop	0.42	0.54	3.07	1.07	0.65	1.04	0.73	1.36	0.67	0.67	0.40	1.08	0.15	0.39	0.54	-	-

1: Ts/(Ts + Tm) (Seifert & Moldowan 1978); 2: diahopane/(diahopane + normoretan) (Cornford *et al.* 1986); *3: 22S/(22S+22R) of C31 17a(H), 21ß(H)-hopanes (Mackenzie et al. 1980); 4: C_{30} hopane/(C_{30} hopane + C_{30} morethane) (Mackenzie et al. 1985); 5: 29Ts/(29Ts + norhopane) (Moldowan et al. 1991); 6: bisnorhopane/(bisnorhopane + norhopane) (Peters & Moldowan 1993); 7: C_{23}-C_{29} tricyclic terpanes/C_{30} aß-hopane (Mello et al. 1988); 8: C_{24} tetracyclic terpane/C_{30} aß-hopane (Mello et al. 1988); 9: sterane/hopane (Mackenzie et al. 1984); 10: ßß/(ßß+aa) of C29 (20R + 20S) sterane isomers (Mackenzie et al. 1980); 11: 20S/(20S + 20R) of C_{29} 5a(H),14a(H),17a(H) sterane isomers (Mackenzie et al. 1984); 12: diasteranes/(diasteranes + regular steranes) (Seifert & Moldowan 1978); 13: % C_{27} of C_{27} + C_{28} + C_{29} ßß-steranes; 14: % C_{28} of C_{27} + C_{28} + C_{29} ßß-steranes; 15: % C_{29} of C_{27} + C_{28} + C_{29} ßß-steranes; 16: C_{20}/(C_{20}+C_{28}) triaromatic steroids (TA) (Mackenzie et al. 1985); 17: C_{28} TA/(C_{28} TA + C_{29} MA) (Mackenzie et al. 1985); 18: methyl phenanthrene ratio, MPR (Radke et al. 1982); 19: methyl phenanthrene index 1, MPI1 (Radke et al. 1982); 20: methyl phenanthrene distribution fraction 1, MPDF (F1) (Kvalheim et al. 1987); 21: methyl dibenzothiophene ratio, MDR (Radke 1988); 22: calculated vitrinite reflection, Rm = 1.1*log10 MPR + 0.95 (Radke 1988); 23: calculated vitrinite reflection, %Rc = 0.60*MPI1 + 0.40 (Radke 1988); 24: calculated vitrinite reflection, %Ro = 2.242*F1 - 0.166 (Kvalheim et al. 1987); 25: calculated vitrinite reflection, Rm = 0.073*MDR + 0.51 (Radke 1988); 26: 3-methyl phenanthrene/4-methyl dibenzothiophene; 27: methyl dibenzothiophenes/methyl phenanthrenes (Radke et al. 2001); 28: pristane/n-heptadecane; 29: phytane/n-octadecane; 30: pristane/phytane; 31: extended tricyclic terpane ratio (ETR) (Holba et al. 2001); 32: C_{28}/C_{29} ßß steranes ratio (Grantham & Wakefield 1988); 33: nordiacholestane ratio (NDR) (Holba et al. 1998); 34: triaromatic dimethylcholesteroid ratio (TA-DMC) (Barbanti et al. 2011).*

ACCEPTED MANUSCRIPT